

Generalized paradox of enrichment: Noise-driven rare rarity in degraded ecological systems

Shirin Panahi¹, Ulrike Feudel², Karen C. Abbott³, Alan Hastings⁴, & Ying-Cheng Lai^{1,5}

¹*School of Electrical, Computer and Energy Engineering, Arizona State University, Tempe, Arizona 85287, USA*

²*Institute for Chemistry and Biology of the Marine Environment, Carl von Ossietzky University Oldenburg, Carl von Ossietzky-Str. 9-11, Oldenburg 26111, Germany*

³*Department of Biology, Case Western Reserve University, 10900 Euclid Avenue, Cleveland, OH 44106, USA*

⁴*Department of Environmental Science and Policy, University of California, One Shields Avenue, Davis, CA 95616, USA and Santa Fe Institute, 1399 Hyde Park Road, Santa Fe, NM 87501, USA*

⁵*Department of Physics, Arizona State University, Tempe, Arizona 85287, USA*

The paradox of enrichment stipulates that increasing the resources available to the prey population can lead to instability and a higher likelihood of population fluctuations. We study the converse situation where the prey's environment is degrading and ask if the dynamical interplay between this degradation and stochasticity can be beneficial to stabilization of the prey population. The underlying systems are nonautonomous and subject to noise. We uncover a phenomenon pertinent to the paradox of enrichment: rare rarity. In particular, in a slow-fast ecosystem with a sole stable equilibrium, noise can induce dynamical excursions of a trajectory into a region with low species abundance, resulting in rarity. Surprisingly, it is the same noise that can facilitate a rapid recovery of the abundance of the rare species, making short the duration of the rarity. As the environment continues to degrade, the occurrence of such rarity events can be nonuniform in time and even more rare. The intermittent occurrence of rare rarity is caused by the dynamical interplay between the phase-space distance from the stable equilibrium to the boundary separating two distinct regions of transient dynamics. The rare-rarity phenomenon can also arise in other natural systems such as the climate carbon-cycle system.

Key words: Paradox of enrichment, species rarity, nonautonomous dynamical systems, transient dynamics

Introduction

Consumer-resource interactions often exhibit cycles of prey over exploitation, crash, and recovery¹. When the prey population's growth capacity is sufficiently low due, for example, to limited

resources or poor habitat quality, these cycles are expected to dampen out over time and the system will approach a stable equilibrium point. However, when the prey's environment is enriched, the equilibrium becomes destabilized with large fluctuations via a supercritical Hopf bifurcation - a local bifurcation where a limit cycle emerges from the equilibrium as the bifurcation parameter changes ². The more favorable conditions allow for a larger and faster prey recovery after over exploitation, resulting in large, sustained oscillations. This phenomenon is known in ecology as the paradox of enrichment: the counterintuitive phenomenon where increasing the availability of resources, such as nutrients in an ecosystem, can lead to instability and a higher likelihood of population fluctuations in consumer-resource systems ³⁻⁹. In this paper, we consider the converse situation where the prey's environment is degrading and ask if the interplay between the direct negative impacts of this degradation and stochasticity might actually lead to the stabilization of the prey population. In particular, we shall demonstrate that the nonlinear dynamical effect of the degradation can lead to species rarity but noise can play the beneficial role of quick recovery, a phenomenon that we call "rare rarity."

Species rarity, referred to as the low abundance of certain species, can arise from multiple mechanisms, each with distinct ecological and dynamical underpinnings. One such mechanism is global climate change, which drives gradual environmental deterioration, progressively reducing population sizes and ultimately leading to rarity ¹⁰⁻¹⁴. Another well-documented pathway to rarity involves tipping-point transitions (e.g., a saddle-node bifurcation), where small environmental changes push the system past a critical threshold, triggering a sudden decline in species abundance ¹⁵⁻²⁸. Additionally, in the neighborhood beyond a supercritical Hopf bifurcation leading to stable oscillations of the population density, at least one population size becomes small for a certain time interval corresponding to transient rarity during the limit cycle. Beyond these well-known mechanisms, species rarity can also emerge from dynamical excursions in slow-fast and excitable systems ²⁹⁻³³. In such cases, rather than exhibiting a gradual decline or an abrupt tipping event, the species abundances temporarily drop as trajectories enter the phase-space regions corresponding to low-density states before recovering. This form of rarity is not necessarily associated with a loss of stability but instead reflects the interplay between intrinsic nonlinear dynamics and external perturbations. Ecological systems are rarely deterministic: they are constantly influenced by stochastic disturbances arising from environmental fluctuations, demographic variability, and external noise ^{24,34-50}. Given its pervasive influence, noise must be considered when investigating species rarity, as it can modulate the frequency, duration, and severity of the rare events. This motivates our study, in which we examine species rarity in a noisy ecological system, focusing on how stochastic effects interact with the underlying deterministic mechanisms to shape rare-rarity events. (Some background topics pertinent to this work are presented in SI Appendix (Sec. I), which include recovery from rarity, tipping, dynamical excursion, noise in ecological systems.)

Previous research in stochastic population dynamics⁵¹, tipping point²² and regime shifts^{52,53} has largely focused on random fluctuations about the stable state or transitions between alternative stable states of the ecosystem. Differing from the existing works, here we investigate transient dynamics in ecosystems with a single globally stable state corresponding to stationary coexistence of predator and prey. More specifically, we present a rarity phenomenon in a noisy slow-fast predator-prey system. The system is subject to continuous parameter change with time caused by, e.g., environmental changes and stochastic disturbances modeled by ecologically realistic demographic noise. In the absence of noise, i.e., in the deterministic case, the parameter changes can cause the system to evolve towards a single dynamical excursion that leads the system into a state, after which the species abundances become near zero, making them rare. The species rarity caused by a dynamical excursion does not represent a permanent shift to an alternative state but rather a temporary departure from the existing one, followed by a quick recovery.

A finding is that, demographic noise that arises commonly in ecological systems can make rare rarity more frequent, resulting in the emergence of an intermittent behavior: the system undergoes an excursion, generating rarity, followed by a fast recovery, and so on. However, due to noise, the time duration in which the system exhibits species rarity is relatively short compared to the time interval between two adjacent rare-rarity events. The excursion-induced rarity is thus rare, effectively preventing extinction. This may be regarded as a kind of resilience of the species. Specifically, in ecology, resilience is understood as the system's ability to return to its original state after a perturbation. Rare rarity introduces a nuanced perspective: while it involves transient excursions to a low-abundance state, such an excursion is followed by a rapid recovery, preventing the population from collapsing in the long run. On average, the species are able to maintain a high abundance level, in spite of occasionally or intermittently becoming rare. The phenomenon of rare rarity is also found in a stochastic carbon-cycle system, suggesting the generality of this phenomenon in nonlinear slow-fast ecological and physical systems.

Results

Slow-fast predator-prey model We consider a variant of the slow-fast Rosenzweig-MacArthur predator-prey system²⁹, subject to demographic noise and parameter variations with time (e.g., as the result of environmental change). For simplicity, we assume that the resources available to the prey species in its habitat decline continuously and linearly with time. The nonautonomous dynamical system subject to multiplicative noise is described by the following set of stochastic

differential equations:

$$\kappa \frac{dx}{dt} = x(1 - \phi x) - \frac{xy}{1 + \eta x} + \xi \sqrt{x} dB(t) \quad (1a)$$

$$\frac{dy}{dt} = \frac{xy}{1 + \eta x} - y + \xi \sqrt{y} dB(t) \quad (1b)$$

$$\frac{d\phi}{dt} = \begin{cases} r, & \phi_{\min} < \phi < \phi_{\max} \\ 0, & \text{otherwise,} \end{cases} \quad (1c)$$

where x and y are the populations of the fast (prey) and slow (predator) species, respectively, $0 < \kappa \ll 1$ quantifies the timescale separation between the prey's and predator's life span, η is the predator's interaction time with the prey, and the term $\xi \sqrt{y} dB(t)$ describes the demographic noise with ξ as the noise amplitude and $dB(t)$ being an independent Gaussian random process of zero mean and unit variance^{42,54}. Let ϕ be the time-dependent bifurcation parameter that is inversely proportional to the carrying capacity of the prey habitat. It varies linearly with time at the rate r from ϕ_{\min} initially to ϕ_{\max} after certain time. As $\phi(t)$ increases with time, the carrying capacity of the prey habitat deteriorates continuously, so $\phi(t)$'s increase with time could, roughly, be the result of the ever increasing human influences on the ecosystem. The three quantities, r , ϕ_{\min} and ϕ_{\max} define a proper or calibrating timescale of the nonautonomous dynamical system (1):

$$T_s \equiv \frac{\phi_{\max} - \phi_{\min}}{r}, \quad (2)$$

with which the duration of various dynamical events of the system can be compared. The quantity T_s is the time interval over which an environmental change is assumed to happen. We integrate the nonautonomous system (1) using a standard second-order method for stochastic differential equations⁵⁵.

Rare rarity in the prey population Figure 1(A) shows the time-varying parameter $\phi(t)$ for $\xi = 0.1$, $r = 0.0002$, $\phi_{\min} = 0.09$, and $\phi_{\max} = 0.199$. All other parameters follow the setting in Ref. [29] with $\eta = 0.8$, and $\kappa = 0.01$. This setting ensures that the system remains in a single globally stable state with stationary coexistence of predator and prey. The corresponding time series of the prey population $x(t)$ is shown in Fig. 1(B). During the time interval in which the control parameter ϕ varies, there are four occurrences of rarity in which the prey population reaches a dangerously low, near-zero level. The remarkable feature is that each occurrence of rarity lasts only for a relatively short time, as exemplified in Fig. 1(C), a magnification of one of the rarity events. The rarity event lasts for a short time in the sense that, in terms of the calibrating time T_s , the duration of the rarity event is less than 1%. Figure 1(C) also shows that, after temporally approaching some near zero value, the prey population quickly recovers to the normal level. Such a rarity event can thus be regarded as a ‘‘quick’’ transient event of temporary population collapse. In the entire observational time interval, the total duration of all rarity events is thus short, rendering

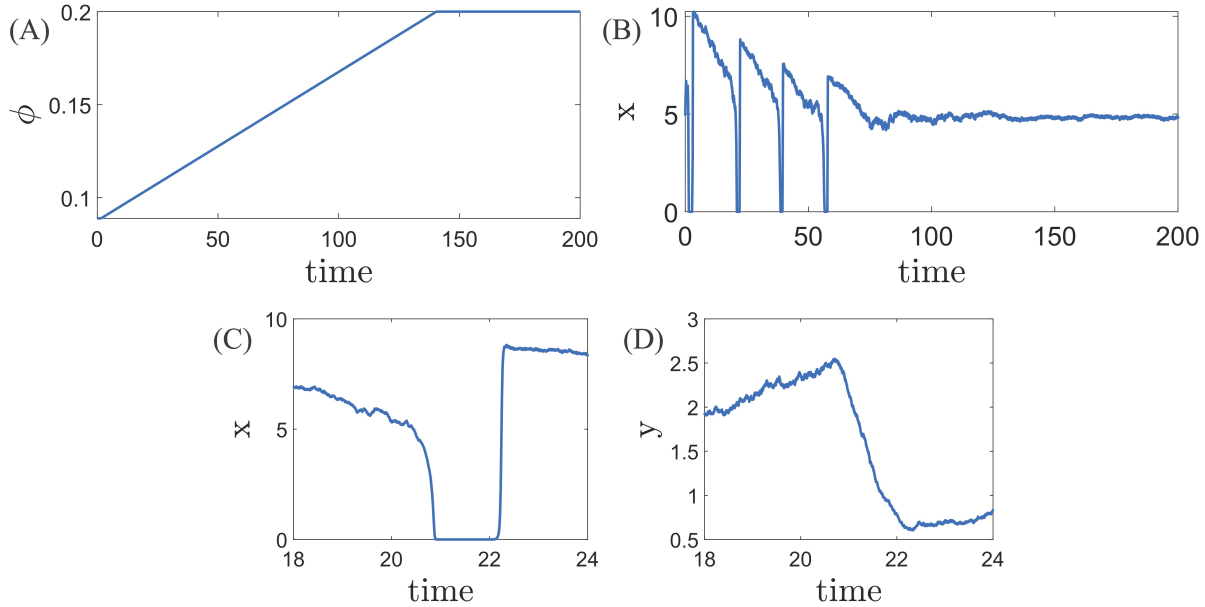


Figure 1: Demonstration of the phenomenon of the rare rarity of the prey population in the nonautonomous predator-prey system (1). (a) Time-varying parameter $\phi(t)$, which is inversely proportional to the carrying capacity and increases linearly from $\phi_{\min} \approx 0.09$ at $t = 0$ to $\phi_{\max} \approx 0.2$ at the rate $r = 0.0002$. (b) A representative time series (a random realization) of the prey population for $\eta = 0.8$ (predator’s interaction time with the prey) and $\kappa = 0.01$ (timescale separation parameter). The amplitude of the demographic noise is $\xi = 0.1$. For this realization, during the time interval in which the capacity parameter ϕ changes, there are four occurrences of the rarity of the prey population. (c) A magnification of a typical rarity event, which lasts for a quite short time relative to the system timescale T_s , signifying “rare rarity.” (d) The corresponding Time series $y(t)$ of the predator population.

rare the rarity events. In fact, the length of the rarity interval is related to the intrinsic timescales of the predator-prey system determined by the parameter κ that characterizes the timescale separation between the lifetimes of the two species: predator and prey. In general, the life spans on different trophic levels follow an allometric slowing down⁵⁶, i.e., species on a higher trophic level (here the predator) grow slower than the species on lower trophic levels (the prey). Note that, in spite of the rare rarity occurrences of the prey population, the predator population maintains at a level well away from zero, as shown in Fig. 1(D).

The time series exemplified in Fig. 1(B) is one random realization of the underlying stochastic dynamical system. To statistically characterize the phenomenon of rare rarity, we define two quantities: (1) ΔT_c , the time interval between two adjacent rare-rarity events, and (2) N_c , the number of occurrences of such events in the time interval $[0, T_s]$. The statistics of the two quantities can be obtained from a large number of dynamical realizations. Figures 2(A) and 2(B) show a his-

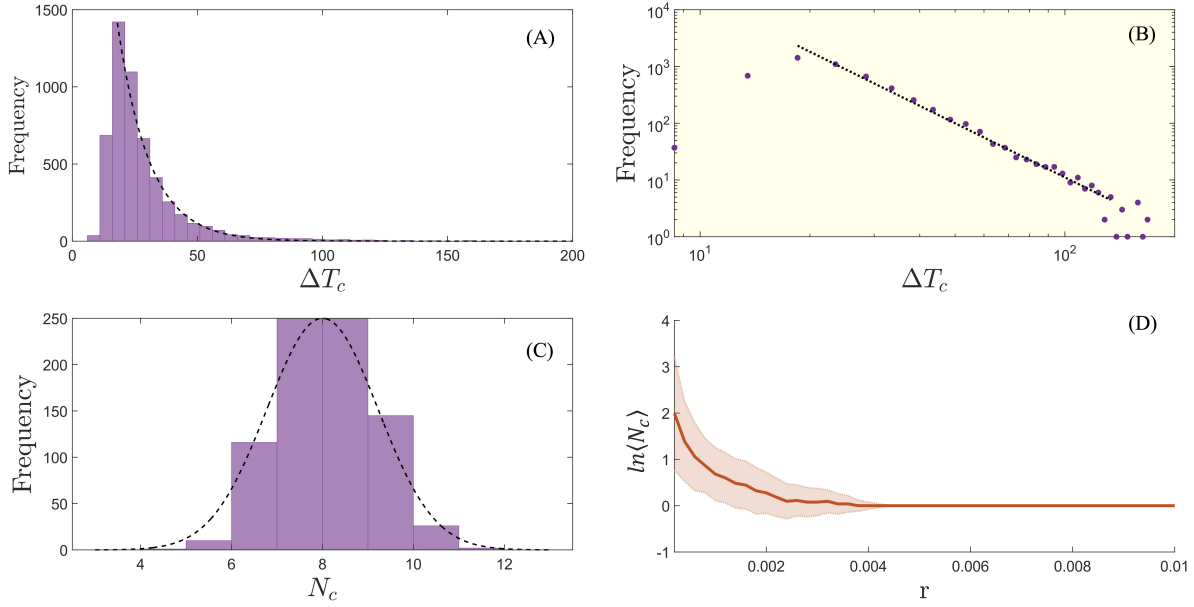


Figure 2: Statistical characterization of rare rarity. (A, B) Distribution of ΔT_c , the time interval between two adjacent rare-rarity events, on a linear and logarithmic scale, respectively, for $r = 0.0002$. (C) Distribution of N_c , the number of rare-rarity events during the time interval of parameter variation for $r = 0.0002$. (D) The mean value $\langle N_c \rangle$ versus the rate of parameter change. Other parameters are the same as in Fig. 1. For clarity, $\langle N_c \rangle$ is plotted on a logarithmic scale, while the shaded area represents the standard deviation on a linear scale.

togram of ΔT_c on a linear and logarithmic scale, respectively, from 800 independent realizations. It can be seen that the distribution of ΔT_c is algebraic or power-law, which is characteristic of typical intermittent behavior in nonlinear dynamical systems⁵⁷. The corresponding histogram of N_c is shown in Fig. 2(C), which is approximately Gaussian with the mean value $\langle N_c \rangle \approx 8$ and variance $\sigma_{N_c} \approx 3$. As the rate r of parameter change increases, on average the number of occurrences of rare rarity decreases, due to the reduction in the time duration T_s of the parameter variation, as shown in Fig. 2(D).

Dynamical mechanism of rare rarity: a deterministic autonomous approach To uncover the dynamical mechanism for the phenomenon of rare rarity as exemplified in Figs. 1 and 2, it is necessary to examine the global phase-space structure²⁹ and study the corresponding autonomous deterministic system of (1) with the bifurcation parameter ϕ :

$$\kappa \frac{dx}{dt} = x(1 - \phi x) - \frac{xy}{1 + \eta x} \quad (3a)$$

$$\frac{dy}{dt} = \frac{xy}{1 + \eta x} - y, \quad (3b)$$

which is a slow-fast system. We choose the value of ϕ from an interval in which both the average prey and predator populations are nonzero. For a perfect timescale separation of predator and prey, $\kappa = 0$, the system (3) can be transformed to slow time t into fast time $\tau = t/\kappa$, leading to

$$\frac{dx}{dt} = x(1 - \phi x) - \frac{xy}{1 + \eta x} \quad (4a)$$

$$\frac{dy}{dt} = \kappa \left(\frac{xy}{1 + \eta x} - y \right), \quad (4b)$$

where the dot now indicates the derivative with respect to τ . The independent variables t and τ correspond to the fast and slow times, with Eqs. (3) and (4) being the fast and slow systems, respectively, which are equivalent for $\kappa \neq 0$. This equation allows us to determine the stability of the critical manifold, which consists of points where the fast dynamics are in an equilibrium, meaning that the fast variables remain constant.

In the limit $\kappa = 0$, the predator population y is constant, and only the fast dynamics of the prey x need to be considered, which can be approximated by a one-dimensional critical manifold (or the x -nullcline of the system) ⁵⁸⁻⁶⁰:

$$M_s = \{(x, y) \in R^2 | x = 0, y = (1 - \phi x)(1 + \eta x)\}, \quad (5)$$

where the first component is a line perpendicular to the fast direction and the second (fold) component is a curve with a fold tangent to the fast direction at the point

$$(x_f, y_f) = ((\eta - \phi)/2\eta\phi, (\eta + \phi)^2/4\eta\phi).$$

To elaborate, the critical manifold M_s consists of the steady states of (4) with $\kappa = 0$, whose stability can be determined. The fold component has a stable and an unstable part with a saddle-node bifurcation at the fold point. The other part of the critical manifold, the y axis as a vertical line, is stable but it becomes unstable below the intersection point with the other part of M_s . This view provides a picture of the direction of the trajectories in that limit, which is only slightly different for $0 < \kappa \ll 1$.

The equilibria of the system (4) are located at the intersections of the x - and y -nullclines. Consider the parameter setting in which the system (3) has one globally stable equilibrium in which the predator and prey coexist. Depending on the initial condition, the slow-fast system exhibits distinct transient behaviors. For example, Figs. 3(A) and 3(B) show two time series of the fast variable from two different initial conditions for $\eta = 0.8$, $\phi = 0.09$, $\kappa = 0.01$, and $\xi = 0.1$. The time series in Fig. 3(A) corresponds to some ‘‘healthy’’ behavior of the prey population in the sense that, in spite of the oscillations, a finite population is maintained. However, for a different initial condition, there is a time interval in which the fast variable approaches zero, as shown in

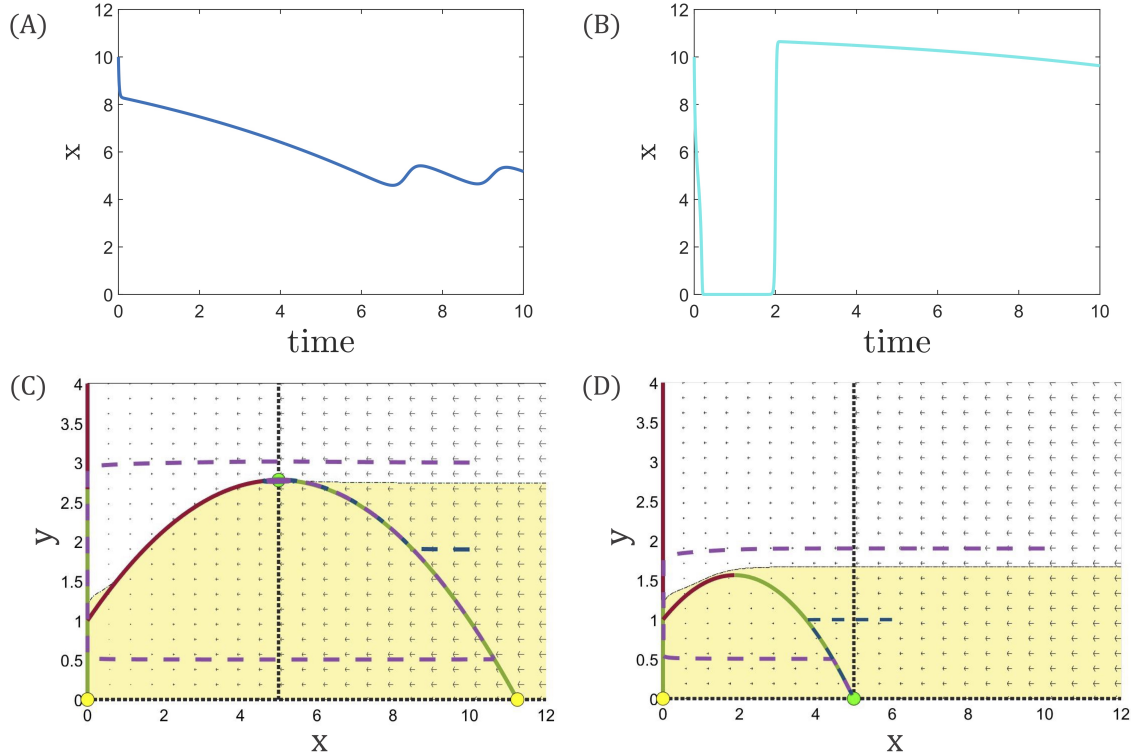


Figure 3: Phase-space structure of the deterministic predator-prey model (3). Two representative time series of the prey population from two different initial conditions: (A) $[10, 2]$ and (B) $[10, 3]$ for $\eta = 0.8$ (redator's interaction time with the prey), $\phi = 0.09$ (inversely proportional to the carrying capacity), $\kappa = 0.01$ (timescale separation parameter), and $\xi = 0.1$ (noise intensity). In (A), the prey population is maintained at a healthy level in the time window of observation. In (B), rarity arises because the prey population becomes near zero for a short transient period of time. (C) Phase-space structure for $\phi = 0.09$, where the white region corresponds to the excursive initial points that undergo temporary collapse of the prey population, leading to rarity, and the initial conditions in the yellow region lead to trajectories that go directly into the sole global stable equilibrium (the filled green circle) without the occurrence of rarity. Since the stable equilibrium is on the boundary between the white and yellow regions, noise with an arbitrary amplitude can land the system into the white region, generating rarity, after which the system settles into stable equilibrium again. This process can repeat, generating the intermittent rarity behavior as exemplified in Fig. 1(B) in the time period in which the control parameter ϕ varies with time but its values are relatively small. (D) Phase-space structure for $\phi = 0.199$. In this case, the stable equilibrium is near the x -axis and is far away from the boundary between the white and yellow regions. While the white region becomes larger as compared with that in (C), noise with an extraordinarily large amplitude is required to kick the system into the white region, making the time to observe such an event prohibitively long, as demonstrated in Fig. 1(B).

Fig. 3(B). The corresponding behavior of rarity lasts for a relatively short period of time before the population recovers to a healthy level. Figure 3(C) shows the phase-space structure of the

system (3) for fixed $\phi = 0.09$ and $\eta = 0.8$, with one globally stable equilibrium (closed green circle) and two unstable equilibria (the two yellow circles). The positions and stability of the equilibria depend on the values of the parameters ϕ and η . The chosen $\phi = 0.09$ is quite close to a supercritical Hopf bifurcation at $\phi = 0.088$, which explains the oscillations for the initial condition visible in Fig. 3(A). The dashed vertical black line represents the y -nullcline. The x -nullcline or the critical manifold of the system is shown by a solid line and curve segments, with the stable (unstable) parts in green (red). The intersection points of the y -nullcline and the critical manifold (x -nullcline) give the equilibria of the system.

Depending on the initial condition, there are two distinct transient behaviors in their convergence to the global stable equilibrium: direct (yellow region) and excursive (white region). For an initial condition from the yellow region, the system approaches the stable equilibrium directly. However, for initial conditions from the excursive region, the system experiences a large excursion in the phase space that includes a close approach to zero populations, leading to a sudden transient collapse in both the predator and prey populations before eventually reaching the stable steady state. Two examples of the dynamical trajectories, one initiated from the white (purple dashed line) and another from the yellow region (blue dashed line), are shown in Fig. 3(C). It can be seen that the dynamical trajectory from the initial condition in the white region approaches the y -axis (zero prey population) and stays near it for a transient period of time before leaving it and approaching the stable equilibrium.

To better understand the state of rarity, we recall that the trajectory rapidly approaches the y -axis when x is near zero. In this regime, the dynamics are effectively governed by the slow variable y alone. A reasonable approximation for the timescale relevant to motion near the y -axis can be obtained by analyzing the associated trajectories. Specifically, by setting $x = 0$ in Eq. (3), we have $\dot{y} = -y$, indicating an exponentially decaying solution. This decay occurs on a timescale much shorter than that of the environmental change. Analyzing the dynamics in fast time $\tau = t/\kappa$ reveals that the intersection of the unstable fold and the y -axis segment of M_s is a critical transition point: it marks where a downward-moving trajectory shifts from being influenced by the stable portion of the critical manifold to being repelled by the unstable part. This repulsion triggers the end of the rarity interval and pushes the system back to a large population density. The degree of attraction to and repulsion from the y -axis is sensitive to the timescale separation parameter κ . Specifically, a larger κ (indicating weaker timescale separation) shortens the duration of rarity while prolonging the escape time. Figure 4(a) illustrates the rarity duration with respect to the timescale separation parameter κ and Fig. 4(b) presents the time evolution of the system for two different values of κ , highlighting its impact on the transient dynamics.

Formally, the basin of attraction of an attractor is the initial conditions whose trajectories

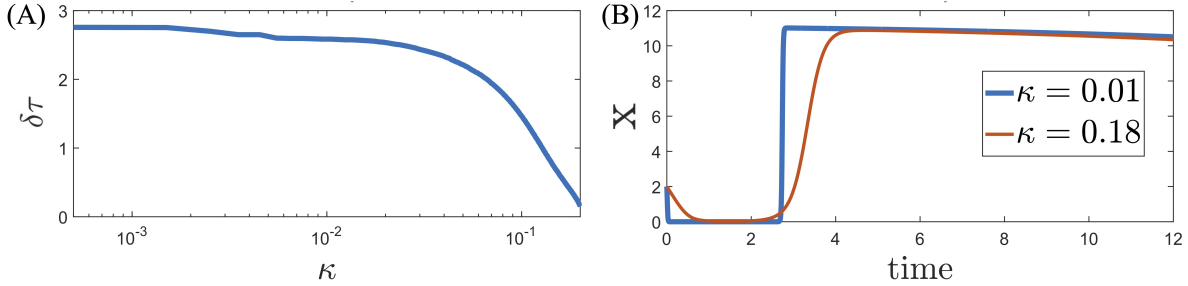


Figure 4: Effect of timescale separation parameter κ on rarity duration. (a) A larger value of κ (smaller timescale separation) results in a shorter period of rarity. (b) Time evolution of the system near the y -axis for two different values of κ : The blue (red) trajectory corresponds to $\kappa = 0.01$ ($\kappa = 0.1$).

eventually reach this attractor^{57,61}. In our work, the dynamics leading to species rarity events demand that the initial conditions whose trajectories exhibit characteristically different behaviors be distinguished, even when they all belong to the same basin of attraction. We thus use the terminology “basin boundary” but only in a loose sense: it does not separate initial conditions that lead to different attractors but rather the initial conditions that follow different trajectories before reaching the same stable attractor. Specifically, our system exhibits a single stable attractor within the relevant ecological parameter range, but initial conditions can evolve along two distinct transient pathways, as illustrated in Figs. 3(C) and 3(D). The smooth boundary separating these two transient regimes defines what is referred to as the “basin boundary.”

The boundary separating the white and yellow region, the “basin boundary” in Figs. 3(C) and 3(D), serve to distinguish initial conditions that follow two distinct types of trajectories: those that initially possess a rarity event and those that do not, before reaching the same stable state. For initial conditions near the deterministic “boundary,” the effect of noise is particularly severe, where small perturbations can push the trajectories from one transient regime to another. Noise thus leads to a probabilistic rather than a sharply defined “basin boundary.” To analyze how this stochastic boundary evolves, we employ Monte Carlo simulations with the following steps: (1) a grid of initial conditions is sampled in the phase space, (2) for each initial condition, multiple noisy realizations of the trajectory are simulated, and (3) the probability $P_A(x_0)$ of a trajectory starting from x_0 following transient pathway A is computed. Figure 5 illustrates the impact of noise on the basin boundary. In particular, Figure 5(A) shows the “boundary” in the deterministic system and Fig. 5(B) presents the stochastic “basin of attraction” for a relatively large noise amplitude ($\xi = 0.1$). Figure 5(C) shows the same basin structure as in Fig. 5(B) but with the white dashed curve included, which represents the deterministic “basin boundary.” It can be seen that the primary effect of noise is blurring the boundary rather than restructuring the basins. In particular, near the

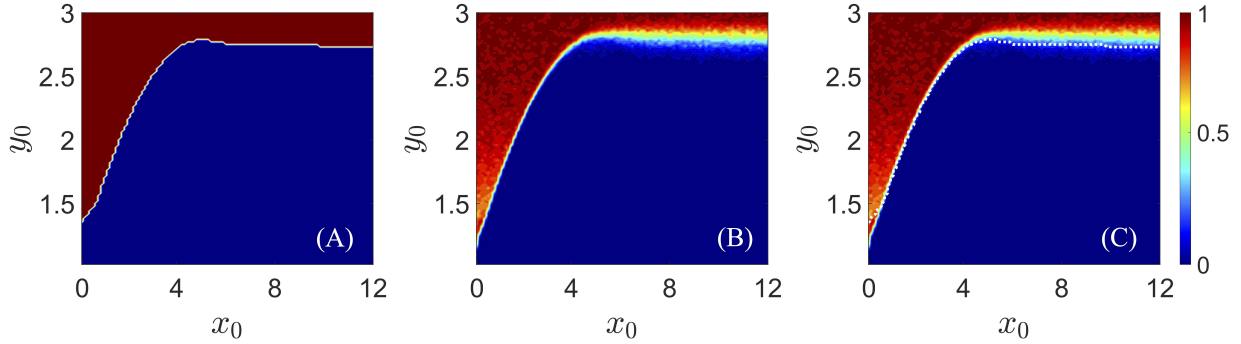


Figure 5: “Basin boundaries” of the predator-prey system. The dark red regions represent the initial conditions that lead to temporary collapses in the prey population, resulting in rarity events. Conversely, initial conditions in the dark blue regions lead to trajectories that directly approach the globally stable equilibrium without such an excursion. (A) “Basin boundary” in the deterministic model. (B) “Basin boundary” under noise of amplitude $\xi = 0.1$. (C) The same basin boundary as in (B) but with the deterministic boundary included (the white dashed curve). All other parameters are the same as those in Fig. 1.

deterministic boundary, noise increases the likelihood of the transitions between the two transient pathways.

The second impact of the noise concerns the time when the intersection point between the two parts of M_s is reached. Due to the closeness to the line of $x = 0$, noise acts mainly on y shifting the point at which the rarity event ends. This shift could occur in either direction (either extending or reducing the duration of prey rarity). However, because the noise has a proportionally larger impact on small populations, noise-driven reductions in y predominate and so the trend is toward shortening the rarity event. But how does the noise amplitude affect the “basin boundary” and the occurrence of rare-rarity events? To address this question, we conduct further simulations using the same parameter values as in Fig. 1 but vary the noise amplitude systematically over five orders of magnitude: from $\xi = 10^{-6}$ to $\xi = 0.1$. For each value of the noise amplitude, we calculate the following key metrics: (1) $\langle \delta\tau \rangle$: the average duration of each rare-rarity event, (2) $\langle \max(\Delta T_c) \rangle$: the average maximum time interval between two consecutive rare-rarity events, and (3) $\langle N_c \rangle$: the average total number of rare-rarity occurrences within a given time window. Each of these quantities is calculated by averaging over 100 realizations of the stochastic system to ensure statistical reliability. The results are summarized in Fig. 6, indicating that varying the noise amplitude can affect the statistical properties of the rare-rarity events but does not eliminate their occurrences. In particular, Fig. 6(a) shows that, as the noise amplitude increases, the average duration $\langle \delta\tau \rangle$ of each rare-rarity event decreases, suggesting that stronger noise perturbs the system more frequently, reducing the persistence of individual rare-rarity occurrences. Figure 6(b)

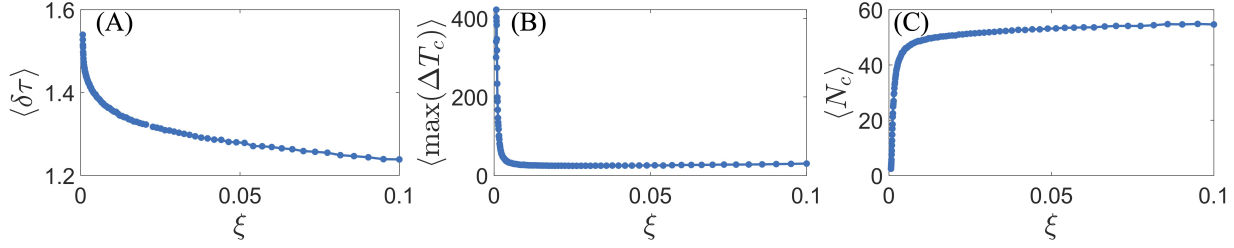


Figure 6: Impact of varying noise amplitude on rare-rarity dynamics. Varying the noise amplitude mainly affect the system’s behavior near the “basin boundary” and the robustness of the rare-rarity phenomenon. The three key metrics characterizing the role of noise in modulating the frequency and persistence of rare-rarity events are: $\langle \delta\tau \rangle$ - the average duration of each rare-rarity event, ΔT_c - the time interval between two consecutive rare-rarity events, and N_c - the total number of rare-rarity occurrences within a given time window. (a) $\langle \delta\tau \rangle$: shorter event duration. As the noise amplitude increases, the average duration $\langle \delta\tau \rangle$ of each rare-rarity event decreases. (b) $\max(\Delta T_c)$: the average maximum time interval between two consecutive rare-rarity events also decreases with increasing noise amplitude. (c) $\langle N_c \rangle$: the total average number of rare-rarity occurrences within a given time window increases with the noise amplitude.

shows that the average time interval $\langle \max(\Delta T_c) \rangle$ between two consecutive rare-rarity events also decreases with increasing noise amplitude, indicating that noise accelerates the transition between the transient pathways, leading to more frequent rare-rarity events. Figure 6(c) shows that the total number $\langle N_c \rangle$ of occurrences increases with the noise amplitude, reinforcing the observation that a stronger stochastic perturbation makes rare-rarity events more frequent. These results suggest that rare rarity is a robust phenomenon, persisting across different noise levels, but its characteristics (frequency, duration, and spacing) depend on the noise amplitude, suggesting the potential of exploiting environmental or ecological fluctuations to modulate the dynamics of rare-rarity events.

Figure 1(B) reveals that for a relatively large value of the bifurcation parameter ϕ , the phenomenon of intermittent rare rarity no longer occurs. This can also be understood by examining the phase-space structure of the deterministic system. Figure 3(D) shows, for $\phi = 0.199$, that the system has a stable equilibrium with a near-zero predator population and an unstable equilibrium corresponding to the extinction of both species. In this case, the folded component of the critical manifold shrinks as compared with the case of a smaller value of ϕ , leading to a larger white area. However, differing from the case of a smaller ϕ value in Fig. 3(C), the global stable equilibrium is now far away from the boundary between the white and yellow regions. Once the system settles into the stable equilibrium, a noise realization of extraordinarily large amplitude is required to kick the system into the white region to exhibit the rarity of the prey population. While abnormally large amplitude realizations are possible for demographic noise, it would require a long time to

actually experience such a realization. This explains why no rarity events occur for large values of ϕ in Fig. 1(B) in the time window of observation. It is worth noting that, for $\phi = 0.199$, the predator population is near zero all the time, as can be seen from Fig. 3(D) which is due to the fact that this point is close to the transcritical bifurcation point ($\phi = 0.2$) where the predator dies out.

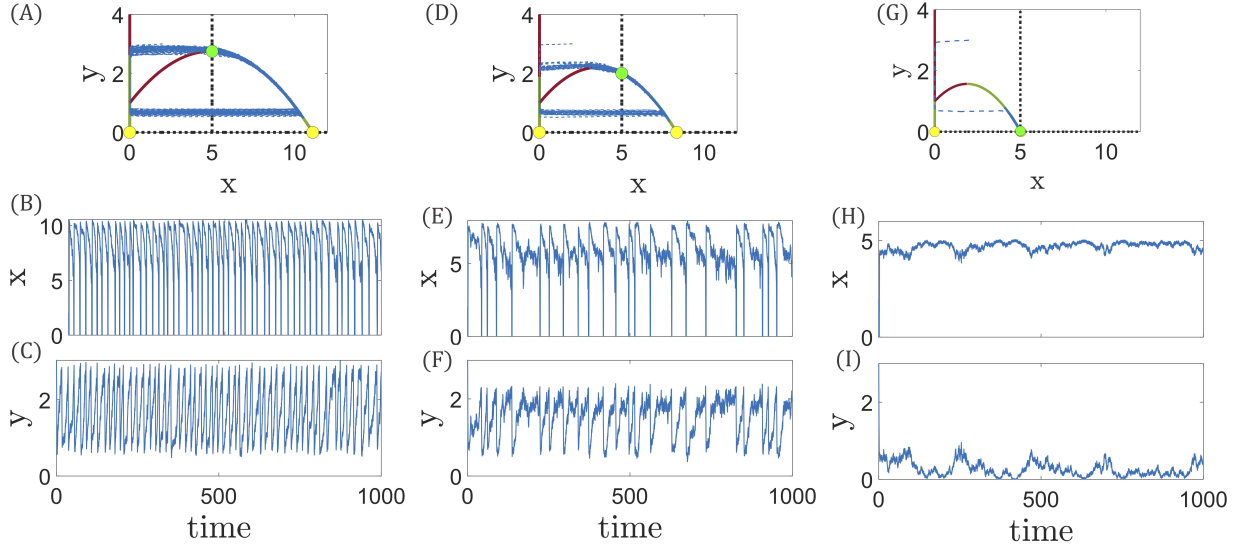


Figure 7: Role of noise in rare rarity. (A-C) Phase-space trajectories and the corresponding time series of the prey population for parameter $\phi = 0.09$ (inversely proportional to the carrying capacity), respectively. The sole stable equilibrium of the system lies close to the boundary between the phase-space regions with distinct transient behavior, so even noise of small amplitude can induce a rare rarity event. (D-F) Same legends as in (A-C) but for $\phi = 0.12$. The stable equilibrium is away from the boundary, requiring larger noise to induce a rare rarity event. This reduces the number of such events in the same time interval as compared with (A-C). (G-I) Same legends as in (A-C) but for $\phi = 0.199$. In this case, the stable equilibrium is far away from the boundary, requiring significantly stronger noise to induce a rare rarity event. No such event occurs in the same time window of observation. Other parameter values are $\eta = 0.8$ (predator's interaction time with the prey), $\kappa = 0.01$ (timescale separation parameter), and $\xi = 0.1$ (noise intensity).

The phase-space structure exemplified in Figs. 3(C) and 3(D) suggests that the distance between the global stable equilibrium and the boundary of the regions with distinct transient dynamical behaviors is key to the occurrence of the rare-rarity events in terms of their frequency and regularity. To verify this explicitly, we compare the trajectories and the corresponding time series of the prey population of the autonomous noisy system for three fixed values of ϕ : $\phi = 0.09$, 0.12 , and 0.199 , in a long time window, as shown in Fig. 7. For $\phi = 0.09$, the stable equilibrium is approximately on the boundary. In this case, even small noise can drive the system out of the equilibrium, leading to a transient excursion in the phase space that stays near the y axis (near zero prey population) for some time, as shown in Figs. 7(A). As a result, the rare-rarity events associated with the prey population occur quite frequently, as shown in Fig. 7(B), which leads to

oscillation in the predator population as depicted in Fig. 7(C). For $\phi = 0.12$, the position of the stable equilibrium is lower in the phase space as compared with the case of $\phi = 0.09$ and is away from the boundary, as shown in Fig. 7(D), so some larger noise is required to induce a rare-rarity event, making these events more infrequent than the case of $\phi = 0.09$, as shown in Fig. 7(E). The predator population and the number of oscillations also decrease as shown in Fig. 7(F). For $\phi = 0.199$, the stable equilibrium is far away from the boundary, so the dynamical trajectory, once approaching the equilibrium, tends to stay there as the required noise level to kick it out is enormous, as shown in Fig. 7(G). In the time window of observation, there is in fact no rare-rarity event, as shown in Fig. 7(H) and the predator population remains near zero without any oscillation, as can be seen from Fig. 7(I).

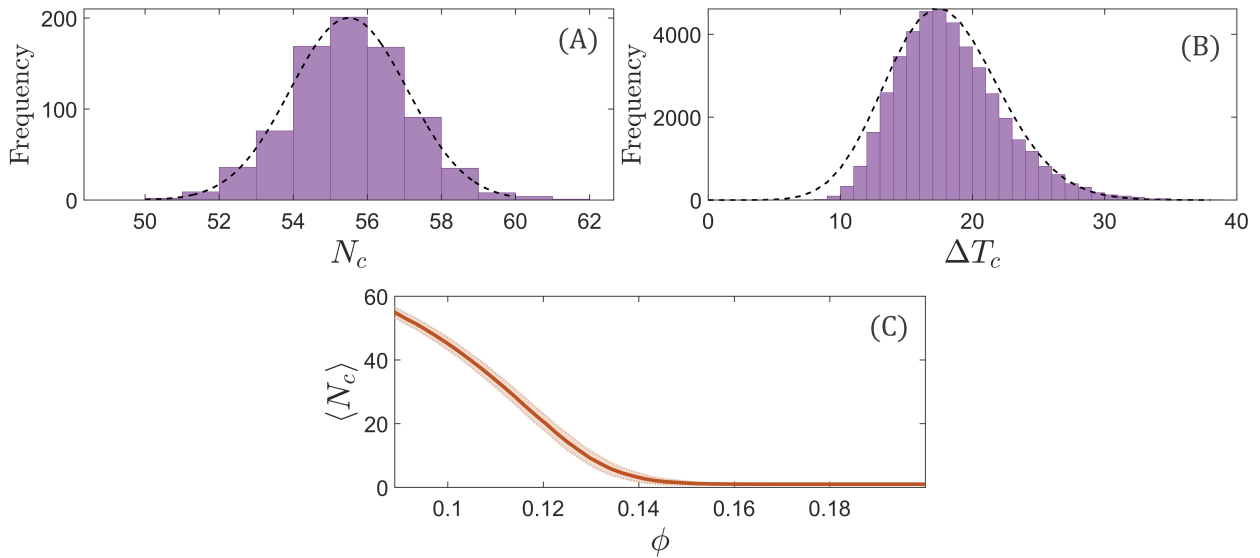


Figure 8: Statistical behavior of rare rarity events in the autonomous system (3) subject to demographic noise. (A) Distribution of N_c , the number of rare rarity events in a long observational time window, which is approximately Gaussian. (B) Distribution of ΔT_c , the time interval between two adjacent rare-rarity events, which is approximately Poisson. The system parameter values are $\phi = 0.09$, $\eta = 0.8$, $\kappa = 0.01$, and $\xi = 0.1$. (C) Average value $\langle N_c \rangle$ of rare rarity events versus ϕ . The shaded area indicates the standard deviation of the average.

Figure 8(A) shows the distribution of the number N_c of the rare rarity events in the time interval $[0, 1000]$ in the autonomous noisy model for $\phi = 0.09$, $\eta = 0.8$, $\kappa = 0.01$, and $\xi = 0.1$, which can be approximated by a normal distribution [similar to that from the nonautonomous system (1) shown in Fig. 2(C)]. Figure 8(B) shows the distribution of ΔT_c , the time interval between two adjacent rare-rarity events, which can be approximated by a Poisson distribution. The most likely time interval between two adjacent rare-rarity events lies in $\Delta T_c \in [16, 18]$. Figure 8(C) shows the mean value of the approximately Gaussian random variable N_c versus the bifurcation

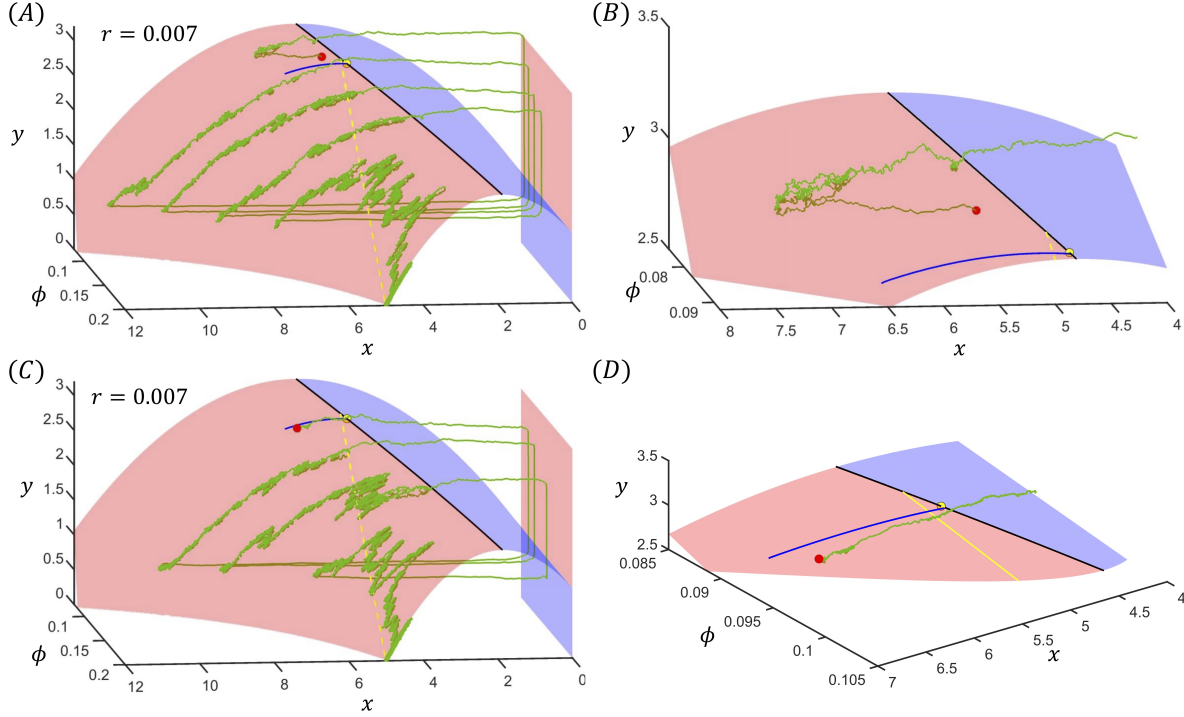


Figure 9: Critical manifold M_s of the nonautonomous system (4) and its stability. The shaded red (blue) region represents the stable (unstable) parts, the moving fold point (x_s, y_s) , and the stable equilibrium is depicted by a solid black line and a dashed yellow line, respectively. The singular canard is represented by a blue trajectory, and the folded saddle singularity is marked by a yellow circle. Green curves illustrate trajectories corresponding to the initial conditions (A) above and (C) below the singular canard (the initial condition is depicted with a red dot). Panels (B) and (D) provide magnified views of (A) and (C), respectively, for clarity.

parameter ϕ where, for each fixed value of ϕ , 800 noisy realizations are used to calculate $\langle N_c \rangle$. The decreasing behavior of $\langle N_c \rangle$ with ϕ is similar to that obtained from the nonautonomous system (1), indicating that species living under poorer environmental conditions (large value of parameter ϕ) tend to retain their abundance and are robust.

Dynamical mechanism of rare rarity: a deterministic nonautonomous approach The final step is to consider the full nonautonomous system with noise (1). Due to the time-dependent change of the environmental conditions with the rate r , all stationary states are transformed into quasistationary equilibria that move in the phase space. For equilibrium state in which predator and prey coexist, we have

$$(x_s, y_s) = (1/1 - \eta, (1 - \eta - \phi(t))/(1 - \eta)^2).$$

Besides the quasistationary state, the critical manifolds M_s as well as the fold (x_f, y_f) change their location in the phase space following the environmental change. For this reason, the situation is more complicated since now not all initial conditions converging to the stable critical manifold without a rarity event will track the quasistationary equilibrium, i.e., stay in its neighborhood during the environmental change. As shown previously²⁹, there are also tipping trajectories that cross the fold and exhibit the collapse-like behavior (excursion), the rarity event. In the phase space, there exists a boundary – a canard trajectory – which separates tracking and tipping trajectories. Now we can have different situations when the noise is acting on those two types of trajectories. A noiseless tipping trajectory can be pushed by the noise over the canard trajectory to make it a trapping trajectory and vice versa. But a tracking trajectory can also be pushed over the fold by the noise. The fourth case could be that the noise prevents tipping. All of those scenarios are possible. We illustrate one of the scenarios by plotting the trajectory shown in Fig. 7 in the full three-dimensional phase space spanned by x , y , and ϕ .

Figure 9 shows two trajectories similar to that one in Fig. 1(B) in 3D including the critical manifold and the canard. The shaded red region represents the stable part of the critical manifold, while the blue area indicates the unstable part. The moving fold point (x_s, y_s) is depicted by a solid black line, and the stable equilibrium is shown with a dashed yellow line. The singular canard is represented by a blue trajectory, and the folded saddle singularity is marked by a yellow circle. Due to the timescale separation, the noise is acting mainly on the critical manifold, not perpendicular to it. The initial conditions for the green trajectory shown in Fig. 9(A) [magnified in Fig. 9(B)] are selected from the upper region of the critical manifold above the critical canard, where the trajectory exhibits a tipping behavior in a noiseless environment. In contrast, the initial conditions for the trajectory in Fig. 9(C) [magnified in Fig. 9(D)] are chosen from the lower region of the critical manifold, in which in a noiseless environment resulting in a trapping behavior. As a result, if the initial condition is chosen from the lower part, noise will first kick the system over the fold, and then the system returns after the rarity event back to the critical manifold but further down as ϕ has changed. It will get pushed by the noise to more rarity events until it ends up too far from the fold where the noise cannot push the system over the fold, as shown in Fig. 1(B).

Carbon-cycle system: positive feedback loop in climate dynamics .

In climate dynamics, a positive feedback loop called the climate-carbon cycle can arise: the release of CO₂ or other greenhouse gases into the atmosphere can increase the global temperature, but the latter can strengthen the climate driving forces that can amplify the CO₂ released into the atmosphere through peat decomposition. The essential nonlinear dynamics governing the feedback phenomenon, also known as the compost-bomb instability, can be modeled by a prototype of a carbon-temperature system proposed in 2011⁶² with the key prediction that the instability depends

strongly on the rate of global warming. Subsequently, this model was found to belong to the general class of the so-called type-B excitable systems¹¹, where an analytical solution indicated that, if the excitable system has a ramping parameter with an asymptotically stable equilibrium and a locally folded critical (slow) manifold, a critical value of the ramping rate can arise, above which an excitable response occurs.

Differing from the ecosystems, here we employ additive noise to illustrate that the phenomenon of rare events is general in fast-slow and excitable systems, regardless of the nature of the noise (i.e., multiplicative or additive). Specifically, we demonstrate that a nonautonomous climate-carbon cycle system subject to environmental noise with a time-varying parameter can exhibit the phenomenon of rare rarity. We consider the carbon-temperature model with the parameter values from Ref.⁶², where global warming is modeled by an atmospheric temperature ramp, as shown in Fig. 10(A). The nonautonomous dynamical system is described by

$$\epsilon \dot{T} = Cr_0 e^{\alpha T} - \frac{\lambda}{A}(T - T_a) + \xi_T^2 \quad (6a)$$

$$\dot{C} = B - Cr_0 e^{\alpha T} + \xi_C^2 \quad (6b)$$

$$\dot{T}_a = \begin{cases} r & \text{if } T_{a_{\min}} < T_a < T_{a_{\max}} \\ 0 & \text{otherwise,} \end{cases} \quad (6c)$$

where C and T are the vertically integrated soil carbon content and soil temperature, respectively, parameter B is the rate of increasing carbon by litter fall from plants and its value can decrease by microbial decomposition proportional to the exponential temperature (we fix $B = 1.055$), $r_0 = 0.02$ is the specific soil respiration rate, $\lambda = 5.049$ is the soil-to-atmosphere heat transfer coefficient, the three scaling parameters are $\alpha = \ln(3.5)/10$, $\epsilon = 0.175$, $A = 39$, and $\xi_{T,C}$ is the noise amplitude. Due to the considerable variation in the timescales of variables, the system described by Eq. (6) can be classified as an extremely stiff system. The pronounced imbalance in the ratio of fast to slow timescales can lead to inherent instability in numerical solutions. This imbalance poses a challenge for standard numerical methods in accurately capturing the dynamics of extremely stiff systems. Consequently, it is necessary to consider specialized techniques or implicit methods to enhance accuracy. In our work, we employ an implicit stochastic Runge–Kutta method^{55,63,64} to integrate the system (6). (The algorithmic details are presented in Sec. S3 of Supplementary Information.)

To be concrete, we assume that the range of temperature variation is $T_{a_{\min}} = 0$ and $T_{a_{\max}} = 10$, as shown in Fig. 10(A). The corresponding time series of $T(t)$ and $C(t)$ are shown in Figs. 10(B) and 10(C), respectively. It can be seen that the carbon concentration $C(t)$ exhibits the phenomenon of rare rarity. Similar to the slow-fast predator-prey system, noise induces intermittent occurrences of rare rarity. For low atmosphere temperatures, multiple rare rarity events can occur in short intervals, leading to potentially catastrophic outcomes. However, as the atmospheric temperature

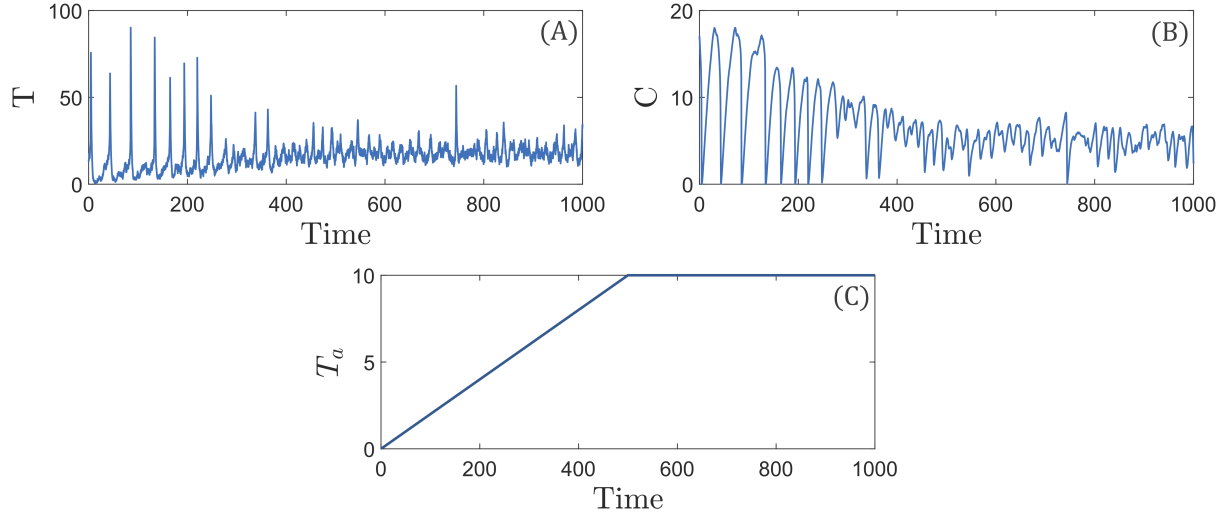


Figure 10: Time trajectory of the nonautonomous system Eq. (6). (A) T (B) C (C) T_a for initial condition $(T_0, C_0, T_{a_0}) = (14, 17, 0)$ for $r = 0.02$, $T_{a_{\min}} = 0$, and $T_{a_{\max}} = 10$.

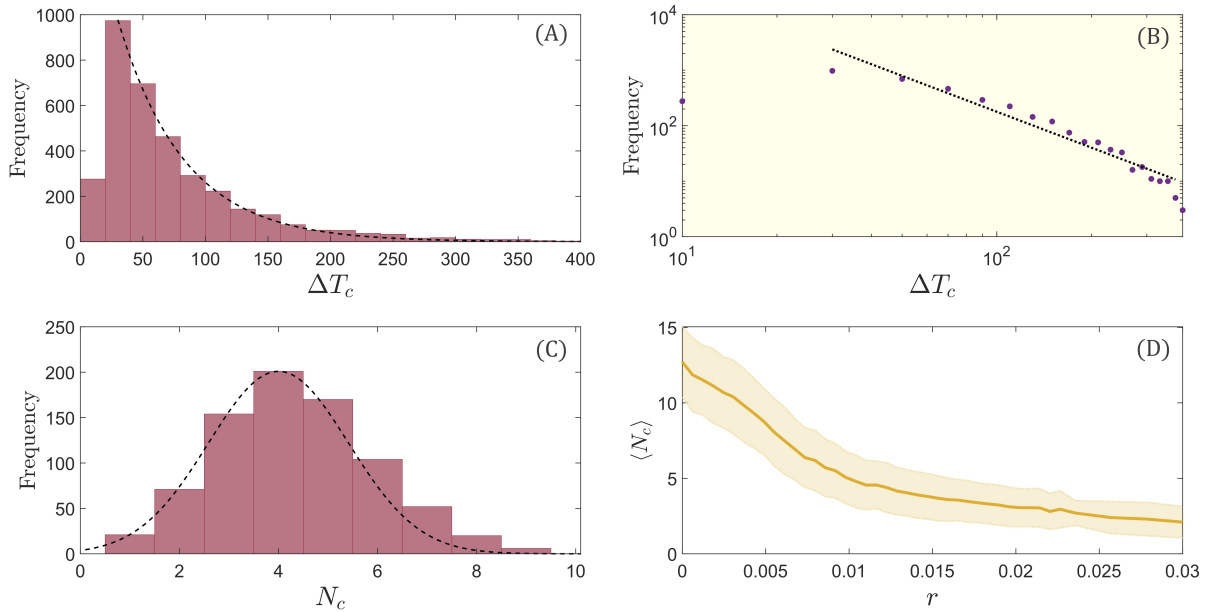


Figure 11: Statistical behaviors of rare rarity events in the climate-carbon cycle system. (A) Distribution of the time interval ΔT_c between two chronologically adjacent rare rarity events and (B) distribution of the number N_c of rare rarity events, for $r = 0.012$, $T_{a_{\min}} = 0$, and $T_{a_{\max}} = 10$. (c) Mean value $\langle N_c \rangle$ of rare rarity events versus r , where the shaded area represents the standard deviation from the average. The larger value of rate r , the smaller number of rare rarity events in the climate-carbon cycle system (6).

increases, there is a decline in the occurrence of such events, resulting in longer intervals between successive events. The distribution of the time interval between two consecutive events is approximately power-law and the number of such events can be modeled as a Gaussian random variable, as shown in Figs. 11(A) and 11(B), respectively. Figure 11(C) shows the mean value $\langle N_c \rangle$ associated with rare rarity events versus the rate r of linear temperature increase. As the atmospheric temperature T_a increases, the compost decomposition becomes more robust to noise, with the probability of experiencing multiple rare rarity events decreasing to near zero. This indicates that global warming can have a significant impact on the dynamics of the climate-carbon cycle system, with higher atmospheric temperatures leading to more robust and stable compost decomposition in the cycle.

In the context of carbon-cycle dynamics, a rarity event represents an unexpected and potentially catastrophic excursive transient behavior that can lead to a drastic reduction in the soil carbon content and a corresponding increase in the emission of carbon into the atmosphere. However, when there is a global warming trend in which the atmospheric temperature T_a increases linearly from $T_{a_{\min}}$ to $T_{a_{\max}}$ at a constant rate r , the number of excursive transient collapses in soil carbon content decrease, accompanied by an increase in the interval between two consecutive rarity events, as exemplified in Figs. 10(B) and 10(C). These findings suggest that, as the atmospheric temperature continues to increase, a reduction in soil carbon content can occur, but the probability of transient collapse reduces as well. The implication is that global warming can counter intuitively enhance the robustness of the climate-carbon cycle against environmental noise. More specifically, as the soil carbon content declines while the noise amplitude remains constant, fewer excursive rare rarity events (compost-bomb instability) are likely to occur. Overall, these results provide insights into the dynamics of the climate-carbon cycle system under different atmospheric temperature conditions, which are relevant to making effective mitigation and adaptation strategies for combating global warming.

Discussion

The dynamical behavior of ecosystems is inherently time-dependent, shaped by persistent environmental and climatic changes, many of which are driven by human activities. As these changes become more systematic and long-term, traditional autonomous models, where system parameters remain fixed, prove insufficient in capturing the evolving nature of ecological systems. Instead, nonautonomous dynamical systems offer a more accurate and necessary framework for modeling ecosystems, allowing for time-dependent variations in key parameters^{11,31,33,65–69}. Moreover, ecosystems are continuously subjected to stochastic influences, including multiplicative demographic noise, which can introduce significant fluctuations in the population dynamics. The interplay between rate-dependent phenomena and stochastic effects has been known to give rise to

counterintuitive dynamical behaviors, including noise-induced and rate-induced tipping points ⁷⁰. Building upon these insights, our study identifies a phenomenon: rare rarity in ecosystems.

Rare rarity occurs when a key ecological variable, such as the abundance of a species, approaches a near-zero value due to a dynamical excursion, rather than through a conventional bifurcation-induced tipping point. This phenomenon emerges in slow-fast and excitable systems, where dynamical trajectories can momentarily visit the phase-space regions containing the near-zero state of a given variable. Unlike the traditional extinction scenarios where a system undergoes a structural change leading to a critical transition, rare rarity events arise due to the interplay between transient dynamics and external perturbations. When noise is present, the dynamical excursions can become intermittent. There are two possible mechanisms that can “kick” the system out of a dynamical excursion (the region close to zero): one is noise and another is the timescale separation between the different components in the slow-fast system. Both mechanisms ensure that rare rarity events remain transient and short-lived relative to the overall timescale of the environmental changes. Notably, the interplay among nonautonomy, noise, and timescale separation creates a double-edged sword: it drives the system into rarity and then rapidly removes it from that state, making rare rarity events exceptionally rare. Furthermore, as a bifurcation parameter evolves over time, the “barrier” for the trajectory to cross to reach the rarity region can become higher, making rarity events even more rare. This explains our counterintuitive result that even when the parameter change is itself detrimental (e.g., degradation of the prey’s carrying capacity), it can protect the population from excursions to rarity. This stabilizing effect is related to the paradox of enrichment, but in reverse.

It is worth noting that similar dynamical excursions occur in other contexts. For example, in neuroscience, neuronal models exhibit subthreshold and superthreshold responses, where small and large excursions reflect a neuron’s reaction to varying stimulus intensities ⁷¹. In climate science and ecology, rate-induced phenomena have been documented, where environmental changes can significantly influence the transient dynamics, potentially leading to an abrupt shift or collapse in the populations ^{31,72}. These examples illustrate how transient excursions, rather than long-term shift in the equilibrium, can lead to certain critical system behavior.

When noise is present, the dynamical excursions can become intermittent. There are two possible mechanisms that can “kick” the system out of dynamical excursion, the region close to zero: one is the noise and another is the timescale separation between the different components in a slow-fast system. Both mechanisms ensure that rare rarity events remain transient and typically short-lived relative to the overall timescale of environmental changes. Notably, the interplay among nonautonomy, noise, and timescale separation creates a double-edged sword: it drives the system into rarity and then rapidly removes it from that state, making rare rarity events exceptionally

rare. Furthermore, as a bifurcation parameter evolves over time, the “barrier” for the trajectory to cross to reach the rarity region can become higher, making rarity events even more rare. This explains our counterintuitive result that even when the parameter change is in itself detrimental (e.g., degradation of the prey’s carrying capacity), it can protect the population from excursions to rarity. This stabilizing effect is related to the paradox of enrichment, but in reverse.

We have demonstrated the existence of rare rarity in two nonautonomous dynamical systems subject to noise: a slow-fast Rosenzweig-MacArthur predator-prey system and a climate-carbon cycle system. Through phase-space analysis of stochastic trajectories, we developed an initial theoretical understanding of this phenomenon. A crucial dynamical feature enabling rare rarity is the presence of a single stable equilibrium. In deterministic excitable systems or slow-fast systems with folded critical manifolds, transient dynamics can lead to two distinct behaviors. In one scenario, trajectories move directly toward the stable equilibrium. In the other, trajectories first undergo an excursion to a different region of phase space, such as a state of near-zero prey abundance in the population dynamics, before eventually settling at the stable equilibrium. The division between these behaviors can be traced back to the initial conditions in two distinct regions, each corresponding to a different transient behavior. The boundary between these regions is the “basin boundary.” The key factor governing the occurrence of rare-rarity excursions is the distance between the stable equilibrium and this “basin boundary.” In the presence of noise, this distance becomes even more critical, as stochastic fluctuations can push trajectories over the boundary, inducing rare-rarity events that would not occur in the purely deterministic setting. As a bifurcation parameter evolves over time, the distance between the stable equilibrium and the basin boundary may either increase or decrease. When this distance is small, even weak noise can trigger rare-rarity excursions, whereas a larger separation requires stronger noise to induce such events. In a non-autonomous system, over time, the occurrence of rarity events follows a nonuniform, intermittent pattern, with their frequency gradually decreasing as time progresses. This reflects the interplay between the system’s intrinsic dynamical structure and the external perturbations shaping its long-term behavior [e.g., Fig. 1(B)].

Besides noise, another key factor in dynamical excursion is timescale separation. Prior research⁷³ investigated the duration of rarity events in a similar predator-prey system with constant parameters and no timescale separation. Without timescale separation, the predator also becomes rare during epochs of prey rarity. As a result, the trajectory passes much more closely in phase space to the saddle points at joint extinction $(0, 0)$ and predator extinction $(1/\phi, 0)$ [the yellow circles in Figs. 3(C), 7(A), and 7(D)]. Because the dynamics slow near saddles, the closer the stochastic trajectory comes to these saddles, the longer it takes for the populations to recover and complete the cycle. Quick recovery from rarity therefore occurs in part due to the slowness of the predator decline, which keeps trajectories from approaching near enough to the $y = 0$ axis to be

trapped in a long transient by the saddle. A key question for future research is determining the threshold of timescale separation necessary for the system to transition from delayed recovery (as in Ref. [73]) to rapid recovery (observed in our study). Investigating this transition could provide additional insights into how ecological systems recover from transient disturbances.

In ecological systems, the relevant source of stochastic influence is often demographic noise and the timescales of the predator and prey variables typically differ drastically. These factors generate the conditions necessary for rare rarity to occur, where the prey population density decreases quickly to a near-zero value, followed by a rapid recovery. This phenomenon arises due to the interplay between noise and the intrinsic slow-fast dynamics of the system coupled to time-dependent environmental changes, illustrating a fundamental mechanism by which species populations can exhibit transient collapse without experiencing true extinction. This suggests that in slow-fast ecological systems, habitat degradation can act as a double-edged sword with both negative and beneficial effects on the prey population. While environmental degradation due to climate change can reduce the overall ecosystem health and cause a decrease in the prey carrying capacity, it also reduces the probability of rare events in the prey population, protecting populations from frequent transient collapses. A similar phenomenon was found in a prototypical excitable climate-carbon cycle system with additive noise, suggesting the generality of the phenomenon.

Author Contributions All conceived the project. SP performed computations and analysis. All analysed data. SP, YCL, and UF wrote the paper. YCL edited the paper.

Acknowledgements and Funding Statement The work was supported by AFOSR under Grant No. FA9550-21-1-0438.

Data Accessibility No empirical data were used in this study. All synthetic data were generated using the computer code available at **Zenodo**: <https://zenodo.org/records/15454597>

Competing Interests The authors declare that they have no competing interests.

Correspondence To whom correspondence should be addressed:
Ying-Cheng.Lai@asu.edu

1. Abbott, K. C. & Dwyer, G. Food limitation and insect outbreaks: complex dynamics in plant–herbivore models. *J. Anim. Ecol.* **76**, 1004–1014 (2007).
2. Hilborn, R. C. *Chaos and Nonlinear Dynamics: An Introduction for Scientists and Engineers* (Oxford university press, 2000).

3. Rosenzweig, M. L. Paradox of enrichment: destabilization of exploitation ecosystems in ecological time. *Science* **171**, 385–387 (1971).
4. Roy, S. & Chattopadhyay, J. The stability of ecosystems: A brief overview of the paradox of enrichment. *J. Biosci.* **1971**, 421–428 (1971).
5. May, R. Limit cycles in predator–prey communities. *Science* **177**, 900–902 (1972).
6. Gilpin, M. & Rosenzweig, M. Enriched predator–prey systems: Theoretical stability. *Science* **177**, 902–904 (1972).
7. Scheffer, M. & De Boer, R. J. Implications of spatial heterogeneity for the paradox of enrichment. *Ecology* **76**, 2270–2277 (1995).
8. Roy, S. & Chattopadhyay, J. The stability of ecosystems: a brief overview of the paradox of enrichment. *J. Biosci.* **32**, 421–428 (2007).
9. Mark, K. *Elements of Mathematical Ecology* (Cambridge University Press, New York, 2001).
10. Thompson, J. M. T. & Sieber, J. Predicting climate tipping as a noisy bifurcation: a review. *Int. J. Bif. Chaos* **21**, 399–423 (2011).
11. Ashwin, P., Wieczorek, S., Vitolo, R. & Cox, P. Tipping points in open systems: bifurcation, noise-induced and rate-dependent examples in the climate system. *Phil. Trans. Roy. Soc. A* **370**, 1166–1184 (2012).
12. Lenton, T. M., Livina, V. N., Dakos, V., van Nes, E. H. & Scheffer, M. Early warning of climate tipping points from critical slowing down: comparing methods to improve robustness. *Phil. Trans. Roy. Soc. A* **370**, 1185–1204 (2012).
13. Barnosky, A. D. *et al.* Approaching a state shift in earth’s biosphere. *Nature* **486**, 52–58 (2012).
14. Lontzek, T. S., Cai, Y.-Y., Judd, K. L. & Lenton, T. M. Stochastic integrated assessment of climate tipping points indicates the need for strict climate policy. *Nat. Clim. Change* **5**, 441–444 (2015).
15. Scheffer, M. *Ecology of Shallow Lakes* (Springer Science & Business Media, 2004).
16. Wysham, D. B. & Hastings, A. Regime shifts in ecological systems can occur with no warning. *Ecol. Lett.* **13**, 464–472 (2010).
17. Drake, J. M. & Griffen, B. D. Early warning signals of extinction in deteriorating environments. *Nature* **467**, 456–459 (2010).

18. Dai, L., Vorselen, D., Korolev, K. S. & Gore, J. Generic indicators for loss of resilience before a tipping point leading to population collapse. *Science* **336**, 1175–1177 (2012).
19. Tylianakis, J. M. & Coux, C. Tipping points in ecological networks. *Trends. Plant. Sci.* **19**, 281–283 (2014).
20. Lever, J. J., Nes, E. H., Scheffer, M. & Bascompte, J. The sudden collapse of pollinator communities. *Ecol. Lett.* **17**, 350–359 (2014).
21. Jiang, J. *et al.* Predicting tipping points in mutualistic networks through dimension reduction. *Proc. Nat. Acad. Sci. (UsA)* **115**, E639–E647 (2018).
22. Jiang, J., Hastings, A. & Lai, Y.-C. Harnessing tipping points in complex ecological networks. *J. R. Soc. Interface* **16**, 20190345 (2019).
23. Scheffer, M. *Critical Transitions in Nature and Society*, vol. 16 (Princeton University Press, 2020).
24. Meng, Y., Jiang, J., Grebogi, C. & Lai, Y.-C. Noise-enabled species recovery in the aftermath of a tipping point. *Phys. Rev. E* **101**, 012206 (2020).
25. Meng, Y., Lai, Y.-C. & Grebogi, C. Tipping point and noise-induced transients in ecological networks. *J. R. Soc. Interface* **17**, 20200645 (2020).
26. Meng, Y., Lai, Y.-C. & Grebogi, C. The fundamental benefits of multiplexity in ecological networks. *J. R. Soc. Interface* **19**, 20220438 (2022).
27. Meng, Y. & Grebogi, C. Control of tipping points in stochastic mutualistic complex networks. *Chaos* **31**, 023118 (2021).
28. O’Keeffe, P. E. & Wicczorek, S. Tipping phenomena and points of no return in ecosystems: beyond classical bifurcations. *SIAM J. Appl. Dyn. Syst.* **19**, 2371–2402 (2020).
29. Vanselow, A., Wicczorek, S. & Feudel, U. When very slow is too fast-collapse of a predator-prey system. *J. Theo. Biol.* **479**, 64–72 (2019).
30. Morozov, A. & Petrovskii, S. Excitable population dynamics, biological control failure, and spatiotemporal pattern formation in a model ecosystem. *Bull. Math. Biol.* **71**, 863–887 (2009).
31. Wicczorek, S., Ashwin, P., Luke, C. M. & Cox, P. M. Excitability in ramped systems: the compost-bomb instability. *Proc. R. Soc. A Math. Phys. Eng. Sci.* **467**, 1243–1269 (2011).
32. Hempson, T. N., Graham, N. A., MacNeil, M. A., Hoey, A. S. & Wilson, S. K. Ecosystem regime shifts disrupt trophic structure. *Ecol. Appl.* **28**, 191–200 (2018).

33. Vanselow, A., Halekotte, L., Pal, P., Wieczorek, S. & Feudel, U. Rate-induced tipping can trigger plankton blooms. *Theo. Ecol.* **17**, 89–105 (2024).
34. Roughgarden, J. A simple model for population dynamics in stochastic environments. *Ame. Naturalist* **109**, 713–736 (1975).
35. Connell, J. H. Diversity in tropical rain forests and coral reefs: high diversity of trees and corals is maintained only in a nonequilibrium state. *Science* **199**, 1302–1310 (1978).
36. Lande, R. Risks of population extinction from demographic and environmental stochasticity and random catastrophes. *Ame. Naturalist* **142**, 911–927 (1993).
37. Yao, Q. & Tong, H. On prediction and chaos in stochastic systems. *Philos. Trans. R. Soc. Lond. A* **348**, 357–369 (1994).
38. Ludwig, D. The distribution of population survival times. *Ame. Naturalist* **147**, 506–526 (1996).
39. Ripa, J., Lundberg, P. & Kaitala, V. A general theory of environmental noise in ecological food webs. *Ame. Naturalist* **151**, 256–263 (1998).
40. Lande, R. Demographic stochasticity and allee effect on a scale with isotropic noise. *Oikos* **83**, 353–358 (1998).
41. Dennis, B. Allee effects in stochastic populations. *Oikos* **96**, 389–401 (2002).
42. Bonsall, M. B. & Hastings, A. Demographic and environmental stochasticity in predator–prey metapopulation dynamics. *J. Animal Ecol.* **73**, 1043–1055 (2004).
43. Ellner, S. P. & Turchin, P. When can noise induce chaos and why does it matter: A critique. *Oikos* **111**, 620–631 (2005).
44. Lai, Y.-C. & Liu, Y.-R. Noise promotes species diversity in nature. *Phys. Rev. Lett.* **94**, 038102 (2005).
45. Lai, Y.-C. Beneficial role of noise in promoting species diversity through stochastic resonance. *Phys. Rev. E* **72**, 042901 (2005).
46. Guttal, V. & Jayaprakash, C. Impact of noise on bistable ecological systems. *Ecol. Model.* **201**, 420–428 (2007).
47. Ruokolainen, L., Lindén, A., Kaitala, V. & Fowler, M. S. Ecological and evolutionary dynamics under coloured environmental variation. *Trends. Ecol. Evol.* **24**, 555–563 (2009).

48. Doney, S. C. & Sailley, S. F. When an ecological regime shift is really just stochastic noise. *Proc. Nat. Acad. Sci. (USA)* **110**, 2438–2439 (2013).
49. Bjornstad, O. N. Nonlinearity and chaos in ecological dynamics revisited. *Proc. Nat. Acad. Sci. (USA)* **112**, 6252–6253 (2015).
50. O'Regan, S. M. How noise and coupling influence leading indicators of population extinction in a spatially extended ecological system. *J. Biol. Dyn.* **12**, 211–241 (2018).
51. Lande, R., Engen, S. & Saether, B.-E. *Stochastic Population Dynamics in Ecology and Conservation* (Oxford University Press on Demand, 2003).
52. Carpenter, S. R. *et al.* Early warnings of regime shifts: A whole-ecosystem experiment. *Science* **332**, 1079–1082 (2011).
53. Scheffer, M., Straile, D., van Nes, E. H. & Houser, H. Climatic warming causes regime shifts in lake food webs. *Limnol. Oceanogr.* **46**, 1780–1783 (2001).
54. Weissmann, H., Shnerb, N. M. & Kessler, D. A. Simulation of spatial systems with demographic noise. *Phys. Rev. E* **98**, 022131 (2018).
55. Van den Broeck, C., Parrondo, J., Toral, R. & Kawai, R. Nonequilibrium phase transitions induced by multiplicative noise. *Phys. Rev. E* **55**, 4084 (1997).
56. West, G. B., Brown, J. H. & Enquist, B. J. A general model for ontogenetic growth. *Nature* **413**, 628–631 (2001).
57. Ott, E. *Chaos in Dynamical Systems* (Cambridge University Press, Cambridge, UK, 2002), second edn.
58. Guckenheimer, J. & Holmes, P. J. *Nonlinear Oscillations, Dynamical Systems, and Bifurcations of Vector Fields* (Springer, New York, 1983).
59. Fenichel, N. Geometric singular perturbation theory for ordinary differential equations. *J. Differ. Equ.* **31**, 53–98 (1979).
60. Ginoux, J.-M. Slow invariant manifolds of slow–fast dynamical systems. *Int. J. Bifurcat. Chaos* **31**, 2150112 (2021).
61. Lai, Y.-C. & Tél, T. *Transient Chaos - Complex Dynamics on Finite Time Scales* (Springer, New York, 2011).
62. Luke, C. & Cox, P. Soil carbon and climate change: from the jenkinson effect to the compost-bomb instability. *Eur. J. Soil Sci.* **62**, 5–12 (2011).

63. Buckwar, E., Rößler, A. & Winkler, R. Stochastic runge–kutta methods for itô sodes with small noise. *SIAM J. Sci. Comput.* **32**, 1789–1808 (2010).
64. Rößler, A. Runge–kutta methods for the strong approximation of solutions of stochastic differential equations. *SIAM J. Numer. Anal.* **48**, 922–952 (2010).
65. Ashwin, P., Perryman, C. & Wieczorek, S. Parameter shifts for nonautonomous systems in low dimension: bifurcation-and rate-induced tipping. *Nonlinearity* **30**, 2185 (2017).
66. Kaszás, B., Feudel, U. & Tél, T. Tipping phenomena in typical dynamical systems subjected to parameter drift. *Sci. Rep.* **9**, 8654 (2019).
67. Jánosi, D., Károlyi, G. & Tél, T. Climate change in mechanical systems: the snapshot view of parallel dynamical evolutions. *Nonlinear Dyn.* **106**, 2781–2805 (2021).
68. Jánosi, D. & Tél, T. Characterizing chaos in systems subjected to parameter drift. *Phys. Rev. E* **105**, L062202 (2022).
69. Feudel, U. Rate-induced tipping in ecosystems and climate: the role of unstable states, basin boundaries and transient dynamics. *Nonlinear Proc. Geophys.* **30**, 481–502 (2023).
70. Slyman, K. & Jones, C. K. Rate and noise-induced tipping working in concert. *Chaos* **33**, 013119 (2023).
71. Markevich, N. & Sel’kov, E. Parametric resonance and amplification in excitable membranes. The Hodgkin-Huxley model. *J. Theor. Biol.* **140**, 27–38 (1989).
72. Ritchie, P. D., Alkhayuon, H., Cox, P. M. & Wieczorek, S. Rate-induced tipping in natural and human systems. *Earth Syst. Dynam* **14**, 669–683 (2023).
73. Rubin, J. E., Earn, D. J., Greenwood, P. E., Parsons, T. L. & Abbott, K. C. Irregular population cycles driven by environmental stochasticity and saddle crawlby. *Oikos* **2023**, e09290 (2023).

Supplementary Information for
Generalized paradox of enrichment: Noise-driven rare rarity in degraded ecological systems

Shirin Panahi, Ulrike Feudel, Karen C. Abbott, Alan Hastings, and Ying-Cheng Lai

Corresponding author: Ying-Cheng Lai (Ying-Cheng.Lai@asu.edu)

CONTENTS

S1. Pertinent background	2
A. Recovery from rarity	2
B. Tipping in ecological systems	2
C. Dynamical excursion in slow-fast and excitable systems	3
D. Noise in ecological systems	3
S2. Carbon-cycle system: positive feedback loop in climate dynamics	3
S3. Stochastic Runge-Kutta Method	6
References	7

S1. PERTINENT BACKGROUND

A. Recovery from rarity

Understanding how rare species avoid extinction is critical for conservation. For species that are chronically rare, persistence has been attributed to factors such as high local abundances (despite very low regional abundance) [1], reproductive adaptations that offset low encounter rates with potential mates [2], and dispersal and niche shifts [3]. For species that only experience rarity during acute collapse events, such as those that we considered in this study, extinction avoidance relies on fast recovery. In single-species populations, this can be accomplished by a high intrinsic growth rate [4]. In multi-species communities, recovery requires not only that the rare species can grow quickly, but that it can do so under the specific pressures being imposed by interacting species [5]. In continually deteriorating environments, rare species must also be able to recover under worse environmental conditions as those that may have caused the collapse to rarity in the first place [6].

B. Tipping in ecological systems

In an ecological system with two coexisting stable equilibria (stable steady states or fixed-point attractors), one associated with healthy survival while the other with extinction, as a parameter changes through a critical point, an inverse saddle-node bifurcation can occur, beyond which the survival attractor no longer exists, leaving the extinction attractor as the only final steady state of the system. This leads to a tipping point at which the species abundances decrease to near-zero values [7–32], which can be considered as below an empirical extinction threshold [33]. Besides population dynamics in ecology, tipping points are relevant to phenomena in other fields such as epidemic outbreak [34], climate change [35], and the sudden switch from normal to depressed mood in bipolar patients [36].

When the parameters of a system vary with time, rate-induced tipping (R-tipping) can occur [16, 37–40]. In particular, for certain initial conditions leading to trajectories approaching the survival equilibrium attractor in the absence of time-dependent parameters, a population with these initial conditions can become extinct if some parameters change too fast with time. The rate of parameter change thus becomes a key “hyperparameter” of the system: as it increases through a critical value, some initial conditions will switch their destination from healthy survival to extinction. It was recognized that the rate of environmental change is effectively a parameter affecting the dynamics across different scales in ecology [41]. In a recent study focusing on complex ecological networks [42], a global approach to R-tipping was introduced with the finding that the probability of R-tipping defined with respect to initial conditions taken from the entire relevant phase-space region can increase rapidly as soon as the rate of parameter changes becomes nonzero. For simple fast-slow systems, one can identify even a boundary in the phase space – a canard trajectory – which separates tipping from tracking (i.e., following the survival state) initial conditions [38, 40, 43]. Besides population dynamics, the phenomenon of R-tipping is relevant to fields such as climate science [44, 45], neuroscience [43, 46], vibration engineering [47], and even competitive economy [48].

C. Dynamical excursion in slow-fast and excitable systems

In ecological systems, another mechanism for rarity can arise in slow-fast [38] and excitable systems [40, 43, 49, 50]. In an early work [49] on a predator-prey model with a Holling type-III predator response, it was found that noise can sustain a transient in the setting that the system has only one globally stable equilibrium. There are two distinct types of trajectories: one that reaches the equilibrium directly and another approaching the equilibrium through an excursive behavior with a sudden but transient excursion away from the equilibrium in both the predator and prey populations. During the excursion, the prey population can reach a near-zero level, resulting in rarity. When noise is present, an intermittent behavior can arise between low-amplitude random oscillations around the equilibrium and the infrequent high-amplitude oscillations away from the equilibrium. In a more recent work [38] on the Rosenzweig-MacArthur predator-prey model, the impact of a specific type of time-dependent parameter change (a linear reduction of the habitat quality over time) on the transient response of the slow-fast dynamics was studied. It was found that a sudden excursion from the stable equilibrium can cause the fast variable (the prey population density) to temporarily collapse to exceedingly low values. Note that R-tipping is not the only mechanism in which transient dynamics can cause regime shifts. It has been shown that transients causing regime shifts are ubiquitous in ecological systems [51–55] with significant management implications [56, 57].

D. Noise in ecological systems

Ecological systems are continually exposed to stochastic disturbances and the effects of noise on the dynamics of these systems have been a topic of study with a long history [28, 58–74]. In general, there are two types of noises in ecological systems: external and internal, where the former can be modeled as additive Gaussian white noise [75, 76] and the latter are demographic or multiplicative noise [59, 66, 71, 77–79]. Demographic noises as a manifestation of internal stochasticity are of particular importance to ecological systems due to the intrinsic uncertainties in reproduction, growth, death, competition, and intraspecific migration. Computationally, a demographic process can be modeled as multiplicative noise with its strength proportional to the square root of the fluctuating abundance. In the context of tipping, the beneficial role of noise in facilitating species recovery after a tipping event was recognized [28, 29].

S2. CARBON-CYCLE SYSTEM: POSITIVE FEEDBACK LOOP IN CLIMATE DYNAMICS

In climate dynamics, a positive feedback loop called the climate-carbon cycle can arise: the release of CO₂ or other greenhouse gases into the atmosphere can increase the global temperature, but the latter can strengthen the climate driving forces that can amplify the CO₂ released into the atmosphere through peat decomposition. The essential nonlinear dynamics governing the feedback phenomenon, also known as the compost-bomb instability, can be modeled by a prototype of a carbon-temperature system proposed in 2011 [80] with the key prediction that the instability depends strongly on the rate of global warming. Subsequently, this model was found to belong to the general class of the so-called type-B excitable systems [16], where an analytical solution indicated that, if the excitable system has a ramped parameter with an asymptotically stable equi-

librium and a locally folded critical (slow) manifold, a critical value of the ramping rate can arise, above which an excitable response occurs.

Differing from the ecosystems, here we employ additive noise to illustrate that the phenomenon of rare events is general in fast-slow and excitable systems, regardless of the nature of the noise (i.e., multiplicative or additive). Specifically, we demonstrate that a nonautonomous climate-carbon cycle system subject to environmental noise with a time-varying parameter can exhibit the phenomenon of rare rarity. We consider the carbon-temperature model with the parameter values from Ref. [80], where global warming is modeled by an atmospheric temperature ramp, as shown in Fig. S1(A). The nonautonomous dynamical system is described by

$$\epsilon \dot{T} = Cr_0 e^{\alpha T} - \frac{\lambda}{A}(T - T_a) + \xi_T^2 \quad (\text{S2.1a})$$

$$\dot{C} = B - Cr_0 e^{\alpha T} + \xi_C^2 \quad (\text{S2.1b})$$

$$\dot{T}_a = \begin{cases} r & \text{if } T_{a_{\min}} < T_a < T_{a_{\max}} \\ 0 & \text{otherwise,} \end{cases} \quad (\text{S2.1c})$$

where C and T are the vertically integrated soil carbon content and soil temperature, respectively, parameter B is the rate of increasing carbon by litter fall from plants and its value can decrease by microbial decomposition proportional to the exponential temperature (we fix $B = 1.055$), $r_0 = 0.02$ is the specific soil respiration rate, $\lambda = 5.049$ is the soil-to-atmosphere heat transfer coefficient, the three scaling parameters are $\alpha = \ln(3.5)/10$, $\epsilon = 0.175$, $A = 39$, and $\xi_{T,C}$ is the noise amplitude. Due to the considerable variation in the time scales of variables, the system described by Eq. (S2.1) can be classified as an extremely stiff system. The pronounced imbalance in the ratio of fast to slow time scales can lead to inherent instability in numerical solutions. This imbalance poses a challenge for standard numerical methods in accurately capturing the dynamics of extremely stiff systems. Consequently, it is necessary to consider specialized techniques or implicit methods to enhance accuracy. In our work, we employ an implicit stochastic Runge–Kutta method [81–83] to integrate the system (S2.1). (The algorithmic details are presented in Appendix S3.)

To be concrete, we assume that the range of temperature variation is $T_{a_{\min}} = 0$ and $T_{a_{\max}} = 10$, as shown in Fig. S1(A). The corresponding time series of $T(t)$ and $C(t)$ are shown in Figs. S1(B) and S1(C), respectively. It can be seen that the carbon concentration $C(t)$ exhibits the phenomenon of rare rarity. Similar to the slow-fast predator-prey system, noise induces intermittent occurrences of rare rarity. For low atmosphere temperatures, multiple rare rarity events can occur in short intervals, leading to potentially catastrophic outcomes. However, as the atmospheric temperature increases, there is a decline in the occurrence of such events, resulting in longer intervals between successive events. The distribution of the time interval between two consecutive events is approximately power-law and the number of such events can be modeled as a Gaussian random variable, as shown in Figs. S2(A) and S2(B), respectively. Figure S2(C) shows the mean value $\langle N_c \rangle$ associated with rare rarity events versus the rate r of linear temperature increase. As the atmospheric temperature T_a increases, the compost decomposition becomes more robust to noise, with the probability of experiencing multiple rare rarity events decreasing to near zero. This indicates that global warming can have a significant impact on the dynamics of the climate-carbon cycle system, with higher atmospheric temperatures leading to more robust and stable compost decomposition in the cycle.

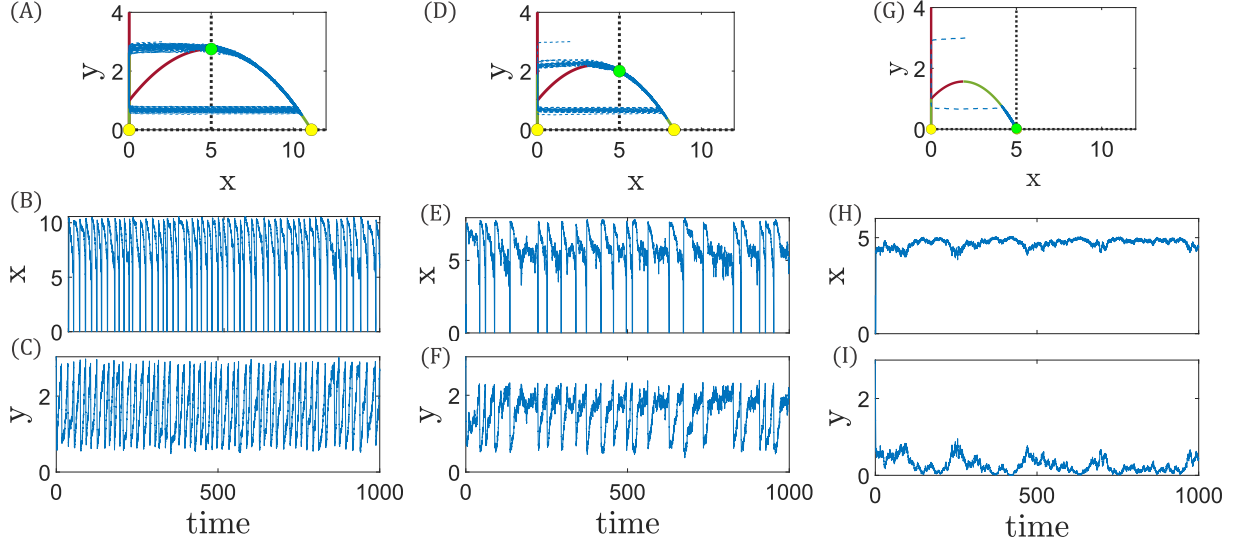


FIG. S1. Time trajectory of the nonautonomous system (S2.1). (A) T_a (B) T (C) C for initial condition $(T_0, C_0, T_{a0}) = (14, 17, 0)$ for $r = 0.02$, $T_{a_{\min}} = 0$, and $T_{a_{\max}} = 10$.

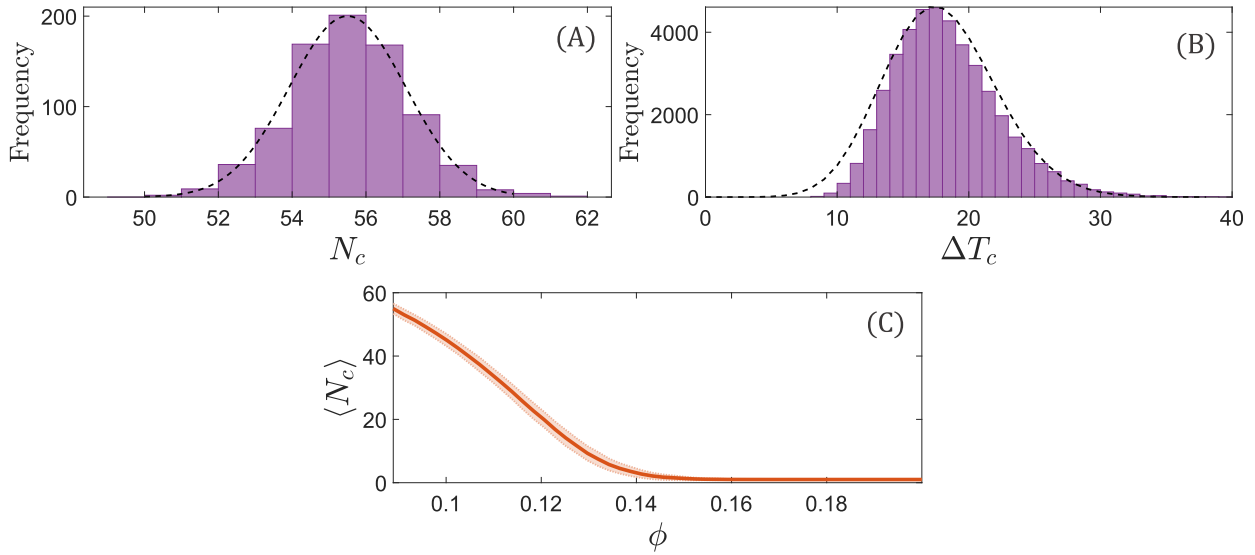


FIG. S2. Statistical behaviors of rare rarity events in the climate-carbon cycle system. (A) Distribution of the time interval ΔT_c between two chronologically adjacent rare rarity events and (B) distribution of the number N_c of rare rarity events, for $r = 0.012$, $T_{a_{\min}} = 0$, and $T_{a_{\max}} = 10$. (c) Mean value $\langle N_c \rangle$ of rare rarity events versus r , where the shaded area represents the standard deviation from the average. The larger value of rate r , the smaller number of rare rarity events in the climate-carbon cycle system (S2.1).

In the context of carbon-cycle dynamics, a rarity event represents an unexpected and potentially catastrophic excursive transient behavior that can lead to a drastic reduction in the soil carbon content and a corresponding increase in the emission of carbon into the atmosphere. However, when there is a global warming trend in which the atmospheric temperature T_a increases linearly from $T_{a_{\min}}$ to $T_{a_{\max}}$ at a constant rate r , the number of excursive transient collapses in soil carbon con-

tent decrease, accompanied by an increase in the interval between two consecutive rarity events, as exemplified in Figs. S1(B) and S1(C). These findings suggest that, as the atmospheric temperature continues to increase, a reduction in soil carbon content can occur, but the probability of transient collapse reduces as well. The implication is that global warming can counter intuitively enhance the robustness of the climate-carbon cycle against environmental noise. More specifically, as the soil carbon content declines while the noise amplitude remains constant, fewer excursive rare rarity events (compost-bomb instability) are likely to occur. Overall, these results provide insights into the dynamics of the climate-carbon cycle system under different atmospheric temperature conditions, which are relevant to making effective mitigation and adaptation strategies for combating global warming.

S3. STOCHASTIC RUNGE-KUTTA METHOD

TABLE S1. Butcher tableau of improved implicit SRK methods (S3.3) - list of coefficients

c_1	a_{11}	a_{12}	\cdots	a_{1s}	b_{11}	b_{12}	\cdots	b_{1s}	
c_2	a_{21}	a_{22}	\cdots	a_{2s}	b_{21}	b_{22}	\cdots	b_{2s}	
\vdots	\vdots	\vdots	\ddots	\vdots	\vdots	\vdots	\ddots	\vdots	
c_s	a_{s1}	a_{s2}	\cdots	a_{ss}	b_{s1}	b_{s2}	\cdots	b_{ss}	
\hat{c}_1	\hat{a}_{11}	\hat{a}_{12}	\cdots	\hat{a}_{1s}					
\hat{c}_2	\hat{a}_{21}	\hat{a}_{22}	\cdots	\hat{a}_{2s}					
\vdots	\vdots	\vdots	\ddots	\vdots					
\hat{c}_s	\hat{a}_{s1}	\hat{a}_{s2}	\cdots	\hat{a}_{ss}					
	β_1	β_2	\cdots	β_s	γ_1	γ_2	\cdots	γ_s	η_1 η_2 \cdots η_s

TABLE S2. Coefficients of improved implicit SRK methods (S3.3) for $s = 2$

$\frac{1}{3}$	$\frac{5}{12}$	$-\frac{1}{12}$	0	0	
1	$\frac{3}{4}$	$\frac{1}{4}$	4	0	
0	0	0			
1	1	0			
	$\frac{3}{4}$	$\frac{1}{4}$	0	1	1 - 1

A nonautonomous dynamical system subject to multiplicative noise can generally be written as

$$\dot{x} = f(x) + \xi(t)g(x), \quad (\text{S3.2})$$

where the deterministic dynamics of the system are described by a d -dimensional nonlinear function $f : R^d \rightarrow R^d$, the second term describes the demographic noise with $\xi(t)$ being a Gaussian random process, and the function $g(x)$ is also a d -dimensional function $g : R^d \rightarrow R^d$. For the climate-carbon cycle model (S2.1), we have $g(x) = 1$.

For nonstiff deterministic differential equations, a commonly used method for solving the corresponding stochastic differential equations (SDE) is some second-order algorithm [81]. However,

if the deterministic equations are stiff, a more robust computational method such as the implicit stochastic Runge-Kutta (SRK) algorithm [82] can be used. Under the Itô–Taylor series expansion, the implicit integration method can be characterized by its extended Butcher tableau. For the case of multidimensional Itô SDEs, the enhanced implicit SRK method is described as

$$\begin{aligned}
x_{n+1} = x_n &+ \sum_{i=1}^s \beta_i f(t_n + c_i \delta t, H_i) \delta t \\
&+ \sum_{i=1}^s \gamma_i g(t_n + \hat{c}_i \delta t, \hat{H}_i) I_r^{\delta t} \\
&+ \sum_{i=1}^s \eta_i g(t_n + \hat{c}_i \delta t, \hat{H}_i) \frac{I_{r_0}^{\delta t}}{\delta t},
\end{aligned} \tag{S3.3}$$

for $n = 0, 1, \dots, N - 1$ with stages:

$$\begin{aligned}
H_i = x_n &+ \sum_{j=1}^s a_{ij} f(t_n + c_j \delta t, H_j) \delta t \\
&+ \sum_{j=1}^s b_{ij} g(t_n + \hat{c}_j \delta t, \hat{H}_j) \frac{I_{r_0}^{\delta t}}{\delta t}
\end{aligned} \tag{S3.4a}$$

$$\hat{H}_i = x_n + \sum_{j=1}^s \hat{a}_{ij} f(t_n + c_j \delta t, H_j) \delta t, \tag{S3.4b}$$

where the increments $I_{r_0, r}$ are the mixed stochastic-classical integrals in the corresponding sub intervals $[t, t + h]$, which can be calculated in the following way. Starting from independent standard normally distributed random variables $\xi_r, \zeta_r \sim N(0, \delta t)$, one computes:

$$I_r = \delta t^{1/2} \xi_r \tag{S3.5}$$

$$I_{r_0} = \delta t^{3/2} (\zeta_r / \sqrt{3} + \xi_r) / 2. \tag{S3.6}$$

The Butcher tableau represents the coefficients of the improved SRK method, where the weights c_i and \hat{c}_i are chosen such that $c = Ae$ and $\hat{c} = \hat{A}e$. The improved SRK method (S3.3) is implicit (explicit) when the matrices A , B , and \hat{A} are full (lower triangular) matrices.

-
- [1] S. Williams, Y. M. Williams, J. VanDerWal, J. L. Isaac, L. P. Shoo, and C. N. Johnson, Ecological specialization and population size in a biodiversity hotspot: how rare species avoid extinction, Proc. Nat. Acad. Sci. (USA) **106**, 19737 (2009).
 - [2] G. J. Vermeij and R. K. Grosberg, Rarity and persistence, Ecol. Lett. **21**, 3 (2018).
 - [3] C. Román-Palacios and J. J. Wiens, Recent responses to climate change reveal the drivers of species extinction and survival, Proc. Nat. Acad. Sci. (USA) **117**, 4211 (2020).
 - [4] R. Lande, Risks of population extinction from demographic and environmental stochasticity and random catastrophes, The American Naturalist **142**, 911 (1993).

- [5] J. L. Sabo and L. R. Gerber, Predicting extinction risk in spite of predator–prey oscillations, *Ecological Applications* **17**, 1543 (2007).
- [6] R. Arumugam, F. Guichard, and F. Lutscher, Persistence and extinction dynamics driven by the rate of environmental change in a predator–prey metacommunity, *Theoretical Ecology* **13**, 629 (2020).
- [7] M. Scheffer, *Ecology of Shallow Lakes* (Springer Science & Business Media, 2004).
- [8] M. Scheffer, J. Bascompte, W. A. Brock, V. Brovkin, S. R. Carpenter, V. Dakos, H. Held, E. H. Van Nes, M. Rietkerk, and G. Sugihara, Early-warning signals for critical transitions, *Nature* **461**, 53 (2009).
- [9] M. Scheffer, Complex systems: foreseeing tipping points, *Nature* **467**, 411 (2010).
- [10] D. B. Wysham and A. Hastings, Regime shifts in ecological systems can occur with no warning, *Ecol. Lett.* **13**, 464 (2010).
- [11] J. M. Drake and B. D. Griffen, Early warning signals of extinction in deteriorating environments, *Nature* **467**, 456 (2010).
- [12] J. M. T. Thompson and J. Sieber, Predicting climate tipping as a noisy bifurcation: a review, *Int. J. Bif. Chaos* **21**, 399 (2011).
- [13] L. Chen, R. Liu, Z.-P. Liu, M. Li, and K. Aihara, Detecting early-warning signals for sudden deterioration of complex diseases by dynamical network biomarkers, *Sci. Rep.* **2**, 342 (2012).
- [14] C. Boettiger and A. Hastings, Quantifying limits to detection of early warning for critical transitions, *J. R. Soc. Interface* **9**, 2527 (2012).
- [15] L. Dai, D. Vorselen, K. S. Korolev, and J. Gore, Generic indicators for loss of resilience before a tipping point leading to population collapse, *Science* **336**, 1175 (2012).
- [16] P. Ashwin, S. Wieczorek, R. Vitolo, and P. Cox, Tipping points in open systems: bifurcation, noise-induced and rate-dependent examples in the climate system, *Phil. Trans. Roy. Soc. A* **370**, 1166 (2012).
- [17] T. M. Lenton, V. N. Livina, V. Dakos, E. H. van Nes, and M. Scheffer, Early warning of climate tipping points from critical slowing down: comparing methods to improve robustness, *Phil. Trans. Roy. Soc. A* **370**, 1185 (2012).
- [18] A. D. Barnosky, E. A. Hadly, J. Bascompte, E. L. B. J. H. Brown, M. Fortelius, W. M. Getz, J. Harte, A. Hastings, P. A. Marquet, N. D. Martinez, A. Mooers, P. Roopnarine, G. Vermeij, J. W. Williams, R. Gillespie, J. Kitzes, C. Marshall, N. Matzke, D. P. Mindell, E. Revilla, and A. B. Smith, Approaching a state shift in earth’s biosphere, *Nature* **486**, 52 (2012).
- [19] C. Boettiger and A. Hastings, Tipping points: From patterns to predictions, *Nature* **493**, 157 (2013).
- [20] J. M. Tylianakis and C. Coux, Tipping points in ecological networks, *Trends. Plant. Sci.* **19**, 281 (2014).
- [21] J. J. Lever, E. H. Nes, M. Scheffer, and J. Bascompte, The sudden collapse of pollinator communities, *Ecol. Lett.* **17**, 350 (2014).
- [22] T. S. Lontzek, Y.-Y. Cai, K. L. Judd, and T. M. Lenton, Stochastic integrated assessment of climate tipping points indicates the need for strict climate policy, *Nat. Clim. Change* **5**, 441 (2015).
- [23] S. Gualdia, M. Tarziaa, F. Zamponic, and J.-P. Bouchaudd, Tipping points in macroeconomic agent-based models, *J. Econ. Dyn. Contr.* **50**, 29 (2015).
- [24] J. Jiang, Z.-G. Huang, T. P. Seager, W. Lin, C. Grebogi, A. Hastings, and Y.-C. Lai, Predicting tipping points in mutualistic networks through dimension reduction, *Proc. Nat. Acad. Sci. (UsA)* **115**, E639 (2018).
- [25] B. Yang, M. Li, W. Tang, S. Liu, Weixinand Zhang, L. Chen, and J. Xia, Dynamic network biomarker indicates pulmonary metastasis at the tipping point of hepatocellular carcinoma, *Nat. Commun.* **9**, 678

- (2018).
- [26] J. Jiang, A. Hastings, and Y.-C. Lai, Harnessing tipping points in complex ecological networks, *J. R. Soc. Interface* **16**, 20190345 (2019).
 - [27] M. Scheffer, *Critical Transitions in Nature and Society*, Vol. 16 (Princeton University Press, 2020).
 - [28] Y. Meng, J. Jiang, C. Grebogi, and Y.-C. Lai, Noise-enabled species recovery in the aftermath of a tipping point, *Phys. Rev. E* **101**, 012206 (2020).
 - [29] Y. Meng, Y.-C. Lai, and C. Grebogi, Tipping point and noise-induced transients in ecological networks, *J. R. Soc. Interface* **17**, 20200645 (2020).
 - [30] Y. Meng and C. Grebogi, Control of tipping points in stochastic mutualistic complex networks, *Chaos* **31**, 023118 (2021).
 - [31] Y. Meng, Y.-C. Lai, and C. Grebogi, The fundamental benefits of multiplexity in ecological networks, *J. R. Soc. Interface* **19**, 20220438 (2022).
 - [32] P. E. O’Keeffe and S. Wieczorek, Tipping phenomena and points of no return in ecosystems: beyond classical bifurcations, *SIAM J. Appl. Dyn. Syst.* **19**, 2371 (2020).
 - [33] R. Gomulkiewicz and R. D. Holt, When does evolution by natural selection prevent extinction?, *Evolution* **49**, 201 (1995).
 - [34] C. Trefois, P. M. Antony, J. Goncalves, A. Skupin, and R. Balling, Critical transitions in chronic disease: transferring concepts from ecology to systems medicine, *Cur. Opin. Biotechnol.* **34**, 48 (2015).
 - [35] K. Albrich, W. Rammer, and R. Seidl, Climate change causes critical transitions and irreversible alterations of mountain forests, *Global Change Biol.* **26**, 4013 (2020).
 - [36] A. Bayani, F. Hadaeghi, S. Jafari, and G. Murray, Critical slowing down as an early warning of transitions in episodes of bipolar disorder: A simulation study based on a computational model of circadian activity rhythms, *Chronobiol. Int.* **34**, 235 (2017).
 - [37] P. Ashwin, C. Perryman, and S. Wieczorek, Parameter shifts for nonautonomous systems in low dimension: bifurcation-and rate-induced tipping, *Nonlinearity* **30**, 2185 (2017).
 - [38] A. Vanselow, S. Wieczorek, and U. Feudel, When very slow is too fast-collapse of a predator-prey system, *J. Theo. Biol.* **479**, 64 (2019).
 - [39] U. Feudel, Rate-induced tipping in ecosystems and climate: the role of unstable states, basin boundaries and transient dynamics, *Nonlinear Proc. Geophys.* **30**, 481 (2023).
 - [40] A. Vanselow, L. Halekotte, P. Pal, S. Wieczorek, and U. Feudel, Rate-induced tipping can trigger plankton blooms, *Theo. Ecol.* **17**, 89 (2024).
 - [41] A. D. Synodinos, R. Karnatak, C. A. Aguilar-Trigueros, P. Gras, T. Heger, D. Ionescu, S. Maaß, C. L. Musseau, G. Onandia, A. Planillo, *et al.*, The rate of environmental change as an important driver across scales in ecology, *Oikos*, e09616 (2022).
 - [42] S. Panahi, Y. Do, A. Hastings, and Y.-C. Lai, Rate-induced tipping in complex high-dimensional ecological networks, *Proc. Nat. Acad. Sci. (USA)* **120**, e2308820120 (2023).
 - [43] S. Wieczorek, P. Ashwin, C. M. Luke, and P. M. Cox, Excitability in ramped systems: the compost-bomb instability, *Proc. R. Soc. A Math. Phys. Eng. Sci.* **467**, 1243 (2011).
 - [44] J. T. Morris, P. Sundareshwar, C. T. Nietch, B. Kjerfve, and D. R. Cahoon, Responses of coastal wetlands to rising sea level, *Ecology* **83**, 2869 (2002).
 - [45] P. D. Ritchie, H. Alkhuon, P. M. Cox, and S. Wieczorek, Rate-induced tipping in natural and human systems, *Earth Syst. Dynam* **14**, 669 (2023).
 - [46] J. Mitry, M. McCarthy, N. Kopell, and M. Wechselberger, Excitable neurons, firing threshold manifolds and canards, *J. Math. Neurosci.* **3**, 1 (2013).

- [47] N. Alexander, O. Oddbjornsson, C. Taylor, H. Osinga, and D. E. Kelly, Exploring the dynamics of a class of post-tensioned, moment resisting frames, *J. Sound Vib.* **330**, 3710 (2011).
- [48] S.-Y. Hsu and M.-H. Shih, The tendency toward a moving equilibrium, *SIAM J. Appl. Dyn. Sys.* **14**, 1699 (2015).
- [49] A. Morozov and S. Petrovskii, Excitable population dynamics, biological control failure, and spatiotemporal pattern formation in a model ecosystem, *Bull. Math. Biol.* **71**, 863 (2009).
- [50] T. N. Hempson, N. A. Graham, M. A. MacNeil, A. S. Hoey, and S. K. Wilson, Ecosystem regime shifts disrupt trophic structure, *Ecol. Appl.* **28**, 191 (2018).
- [51] A. Hastings and K. Higgins, Persistence of transients in spatially structured ecological models, *Science* **263**, 1133 (1994).
- [52] A. Hastings, Transient dynamics and persistence of ecological systems, *Ecol. Lett.* **4**, 215 (2001).
- [53] A. Hastings, Transients: the key to long-term ecological understanding?, *Trends Ecol. Evol.* **19**, 39 (2004).
- [54] A. Hastings, K. C. Abbott, K. Cuddington, T. Francis, G. Gellner, Y.-C. Lai, A. Morozov, S. Petrovskii, K. Scranton, and M. L. Zeeman, Transient phenomena in ecology, *Science* **361**, eaat6412 (2018).
- [55] A. Morozov, K. Abbott, K. Cuddington, T. Francis, G. Gellner, A. Hastings, Y.-C. Lai, S. Petrovskii, K. Scranton, and M. L. Zeeman, Long transients in ecology: theory and applications, *Phys. life Rev.* **32**, 1 (2020).
- [56] A. Hastings, Timescales and the management of ecological systems, *Proc. Nat. Acad. Sci. (USA)* **113**, 14568 (2016).
- [57] T. Francis, K. Abbott, K. Cuddington, G. Gellner, A. Hastings, Y.-C. Lai, A. Morozov, S. Petrovskii, and M. L. Zeeman, Management implications of long transients in ecological systems, *Nat. Ecol. Evol.* **5**, 285 (2021).
- [58] J. Roughgarden, A simple model for population dynamics in stochastic environments, *Ame. Naturalist* **109**, 713 (1975).
- [59] J. H. Connell, Diversity in tropical rain forests and coral reefs: high diversity of trees and corals is maintained only in a nonequilibrium state., *Science* **199**, 1302 (1978).
- [60] R. Lande, Risks of population extinction from demographic and environmental stochasticity and random catastrophes, *Ame. Naturalist* **142**, 911 (1993).
- [61] Q. Yao and H. Tong, On prediction and chaos in stochastic systems, *Philos. Trans. R. Soc. Lond. A* **348**, 357 (1994).
- [62] D. Ludwig, The distribution of population survival times, *Ame. Naturalist* **147**, 506 (1996).
- [63] J. Ripa, P. Lundberg, and V. Kaitala, A general theory of environmental noise in ecological food webs, *Ame. Naturalist* **151**, 256 (1998).
- [64] R. Lande, Demographic stochasticity and allee effect on a scale with isotropic noise, *Oikos* **83**, 353 (1998).
- [65] B. Dennis, Allee effects in stochastic populations, *Oikos* **96**, 389 (2002).
- [66] M. B. Bonsall and A. Hastings, Demographic and environmental stochasticity in predator–prey metapopulation dynamics, *J. Animal Ecol.* **73**, 1043 (2004).
- [67] S. P. Ellner and P. Turchin, When can noise induce chaos and why does it matter: A critique, *Oikos* **111**, 620 (2005).
- [68] Y.-C. Lai and Y.-R. Liu, Noise promotes species diversity in nature, *Phys. Rev. Lett.* **94**, 038102 (2005).
- [69] Y.-C. Lai, Beneficial role of noise in promoting species diversity through stochastic resonance, *Phys.*

- Rev. E **72**, 042901 (2005).
- [70] V. Guttal and C. Jayaprakash, Impact of noise on bistable ecological systems, *Ecol. Model.* **201**, 420 (2007).
 - [71] L. Ruokolainen, A. Lindén, V. Kaitala, and M. S. Fowler, Ecological and evolutionary dynamics under coloured environmental variation, *Trends. Ecol. Evol.* **24**, 555 (2009).
 - [72] S. C. Doney and S. F. Sailley, When an ecological regime shift is really just stochastic noise, *Proc. Nat. Acad. Sci. (USA)* **110**, 2438 (2013).
 - [73] O. N. Bjornstad, Nonlinearity and chaos in ecological dynamics revisited, *Proc. Nat. Acad. Sci. (USA)* **112**, 6252 (2015).
 - [74] S. M. O'Regan, How noise and coupling influence leading indicators of population extinction in a spatially extended ecological system, *J. Biol. Dyn.* **12**, 211 (2018).
 - [75] M. Heino, Noise colour, synchrony and extinctions in spatially structured populations, *Oikos* **83**, 368 (1998).
 - [76] T. G. Benton, C. Lapsley, and A. P. Beckerman, The population response to environmental noise: population size, variance and correlation in an experimental system, *J. Animal Ecol.* **71**, 320 (2002).
 - [77] B. T. Grenfell, O. N. Bjornstad, and B. F. Finkenstädt, Dynamics of measles epidemics: Scaling noise, determinism, and predictability with the tsir model, *Ecol. Monographs* **72**, 185 (2002).
 - [78] P. V. Martín, J. A. Bonachela, S. A. Levin, and M. A. Muñoz, Eluding catastrophic shifts, *Proc. Nat. Acad. Sci. (USA)* **112**, E1828 (2015).
 - [79] G. W. A. Constable, T. Rogers, A. J. McKane, and C. E. Tarnita, Demographic noise can reverse the direction of deterministic selection, *Proc. Nat. Acad. Sci. (USA)* **113**, E4745 (2016).
 - [80] C. Luke and P. Cox, Soil carbon and climate change: from the jenkinson effect to the compost-bomb instability, *Eur. J. Soil Sci.* **62**, 5 (2011).
 - [81] C. Van den Broeck, J. Parrondo, R. Toral, and R. Kawai, Nonequilibrium phase transitions induced by multiplicative noise, *Phys. Rev. E* **55**, 4084 (1997).
 - [82] E. Buckwar, A. Rößler, and R. Winkler, Stochastic runge–kutta methods for itô sodes with small noise, *SIAM J. Sci. Comput.* **32**, 1789 (2010).
 - [83] A. Rößler, Runge–kutta methods for the strong approximation of solutions of stochastic differential equations, *SIAM J. Numer. Anal.* **48**, 922 (2010).